The Journal of Neuroscience, July 1994, 14(7): 4412–4432

Activation of K Current in the Accessory Radula Closer Muscle of *Aplysia californica* by Neuromodulators That Depress Its Contractions

V. Březina,[1] C. G. Evans,[1] and K. R. Weiss[1,2]

[1]Department of Physiology and Biophysics and the [2]Fishberg Research Center in Neurobiology, Mount Sinai School of Medicine, New York, New York 10029

The neural and cellular mechanisms of plasticity apparent in the feeding behavior of the mollusk *Aplysia californica* have been extensively studied in a simple neuromuscular circuit consisting of the accessory radula closer (ARC) muscle and its innervating motor and modulatory neurons. In this circuit, the plasticity is largely due to modulation of the amplitude and duration of the contractions of the muscle by a variety of modulatory neurotransmitters and peptide cotransmitters, among them the small cardioactive peptides (SCPs), myomodulins (MMs), and serotonin (5-HT). We have studied dissociated but functionally intact ARC muscle fibers to determine whether modulation of membrane ion currents in the muscle might underlie these effects. Using voltage-clamp techniques, we found that two currents were indeed modulated. In the preceding article, we proposed that enhancement of "L"-type Ca current is the mechanism by which the modulators potentiate the amplitude of ARC-muscle contractions. Here, we report that the modulators also activate a distinctive K current. Large K currents were activated, in particular, by MM_A, while MM_B, the SCPs, and 5-HT activated much smaller currents most likely of the same kind. Buccalins, modulators that do not act directly on the ARC muscle, were ineffective. The modulator-induced K current was strongly enhanced by depolarization, but relatively slowly so that its amplitude continued to increase for several hundred milliseconds following a depolarizing voltage step. The current was Ca^{2+} independent, not readily blocked by extracellular Cs^+ or Ba^{2+} and only by high concentrations of tetraethylammonium. However, it was almost completely blocked by as little as 10 μM 4-aminopyridine. In contrast to the modulator-induced enhancement of Ca current, activation of the K current was not significantly mimicked by elevation of cAMP. In the intact as well as the dissociated ARC muscle, although low levels of all of the modulators potentiate contractions, even moderate levels of MM_A strongly depress them, whereas the other modulators depress them weakly only at high concentrations. The modulator-induced K current appears well suited to counteract depolarization of the muscle and thus limit activation of the "L"-type Ca current that provides Ca^{2+} essential for contraction. We therefore propose that the modulators depress ARC-muscle contractions in large part by activating the K current. This occurs simultaneously with the enhancement of the Ca current; net potentiation or depression then depends on the balance between the relative strengths of the modulation of the two ion currents.

[Key words: neuropeptides, cotransmitters, neuromodulators, smooth muscle, membrane ion channels, potassium current, mollusk,* Aplysia *]

In the introductory remarks to the preceding article (Březina et al., 1994d), we have already reviewed the current understanding of the *Aplysia* accessory radula closer (ARC)-muscle system, with particular emphasis on the variety of modulatory transmitters and peptide cotransmitters whose actions are likely to be important mechanisms regulating the physiological and behavioral output of the system. Here we shall recapitulate only several facts essential for understanding the work described in this article. The ARC muscle contracts when it is depolarized by ACh, the "classical" transmitter released by its two motor neurons B15 and B16 (Cohen et al., 1978). However, these neurons contain also numerous peptide cotransmitters of several different families, including the small cardioactive peptides (SCPs), myomodulins (MMs), and buccalins (Cropper et al., 1987a,b, 1988, 1990, 1991a; Vilim et al., unpublished observations). In addition, the metacerebral cells (MCCs) release serotonin (5-HT; Weiss et al., 1978). These agents modulate the amplitude and duration of the ACh-induced contractions. The buccalins appear to act presynaptically by altering the release of ACh from the motor neurons (Cropper et al., 1988, 1990), but the SCPs, MMs, and 5-HT act powerfully on the postsynaptic ARC muscle itself. At low concentrations, these postsynaptic modulators all potentiate the amplitude of the contractions (Weiss et al., 1978; Lloyd et al., 1984; Cropper et al., 1987b, 1988, 1991a). With increasing concentration, the SCPs, 5-HT, and some of the MMs such as MM_B remain potentiators; weak depression of the contractions is sometimes observed only at very high concentrations (E. C. Cropper, personal communication). MM_A, in contrast, begins to depress the contractions already above 10^{-7} M (Cropper et al., 1991a).

This article is the fifth part of our study of the electrophysiology of dissociated ARC muscle fibers undertaken to test the hypothesis that the postsynaptic modulators alter the contrac-

Received Sept. 23, 1993; revised Jan. 19, 1994; accepted Jan. 27, 1994.

We thank Mr. J. A. Kozak for helping perform several experiments reported here. This work was funded by NIMH (MH36730 to K.R.W. and K21 MH00987 to V.B.), the McKnight Foundation (K.R.W.), the Revson Foundation (V.B.), and the Whitehall Foundation (V.B.).

Correspondence should be addressed to Dr. V. Březina, Department of Physiology and Biophysics, Box 1218, Mt. Sinai School of Medicine, 1 Gustave L. Levy Place, New York, NY 10029.

tions of the ARC muscle by modulating its membrane ion currents. In the first three articles (Březina et al., 1994a–c), we characterized the major ion currents present in the unmodulated fibers and their likely roles in normal contraction. In the preceding article (Březina et al., 1994d), we reported that the modulators enhance one of the currents, the "L"-type Ca current, and proposed this as a mechanism of the potentiation of the contractions. We also reported and discussed findings indicating that the dissociated fibers remain functionally intact; most importantly, their contractions, just like those of the whole ARC muscle, were potentiated by 5-HT and SCP_B, and often potentiated but also sometimes strongly depressed by MM_A.

This last effect is the subject of this article. We describe here a second effect of the modulators, particularly MM_A, on a membrane ion current in the ARC muscle fibers, activation of a K current that, we propose, is a major mechanism of the depression of contractions.

An abstract of this work has appeared (Březina et al., 1992).

Materials and Methods

The methods used in these experiments were essentially those described in detail in the first article in this series (Březina et al., 1994a) and summarized in the preceding article (Březina et al., 1994d). Very briefly, single fibers dissociated from the ARC muscle were embedded in the top layer of an agarose gel for mechanically stable recording. Solution was continuously superfused over the gel throughout the experiment. All indications were that the gel did not appreciably slow access to the embedded fibers by substances even as large as the peptide modulators added to the superfused solution (see Materials and Methods of Březina et al., 1994a,d). Nevertheless, this access rate was probably the primary determinant of the time courses of most of the effects of drugs and modulators described in this article, most importantly the speed of development of the modulator-induced K current (e.g., Fig. 1*B*). The fibers were impaled with one or sometimes two sharp intracellular microelectrodes, and voltage clamped using either the discontinuous single-electrode (SEVC) or the two-electrode technique.

Voltage-clamp protocols. We studied the modulator-induced K current in one of three ways.

(1) Most often, we applied slow voltage ramps to generate current–voltage (*I–V*) relations regularly every 10 sec (e.g., Fig. 1*A*), or in early experiments every 60 sec (Fig. 1*C*), before and during application of the modulator. Standard ramps swept the voltage from nominally −100 to −30 mV at 14 mV/sec. In the first article in this series, we found that such ramps yielded essentially steady state *I–V* relations of the basal, unmodulated currents present in the ARC muscle fibers at these voltages (Březina et al., 1994a). They appeared to yield steady state *I–V* relations also of the modulator-induced current. Thus, after development of even the large MM_A-induced current (see Results), identical *I–V* relations were obtained with ramps somewhat slower or faster than 14 mV/sec, and with ramps given every 10, 20, or 60 sec. Furthermore, plotting the current flowing at a particular voltage during successive ramps yielded an essentially identical time course of development and desensitization of the modulator-induced current as holding the membrane continuously at that voltage (compare, e.g., Fig. 1*Ac,B*). Desensitization of the modulator-induced current was slow relative to the 10 sec interramp interval (Fig. 1*Ac*). Finally, while the modulator-induced current was strongly voltage dependent (enhanced by depolarization; see Results), voltage steps showed that it reequilibrated at a new voltage within 100–200 msec (see Fig. 12*A*) and thereafter maintained a constant amplitude, with no further increase or decrease (i.e., no voltage-dependent inactivation) during steps as long as 5 sec (see Fig. 12*B*). Since the kinetics of the current were fast compared to the standard 14 mV/sec voltage-ramp speed, the current was presumably near steady state throughout the ramp.

As already mentioned, we often extracted the time course of the modulator effect from the series of *I–V* relations by constructing a running plot of the current flowing at a particular voltage during successive ramps (e.g., Fig. 1*Ac,Cb*). We routinely chose the voltage at which the modulator-induced current was largest; occasionally this was some voltage in the middle of ramp range such as −70 mV (Fig. 1*C*), but in the great majority of cases it was the voltage at the positive end of the ramp (Fig. 1*A*). Nominally, this was −30 mV, but due to the relatively high resistance of our microelectrodes and the limited voltage-clamp gain of the SEVC, there was often some steady state error between the nominal (commanded) and the actual voltage (see Březina et al., 1994a). The error increased with the amplitude of the current being clamped, so that ramps after development of the modulator-induced current often failed to attain the nominal −30 mV by a significantly larger amount than the ramps before (e.g., Fig. 1*Aa*). For convenience, we nevertheless continued to plot the end-ramp current, somewhat underrepresenting the true amplitude of the modulator-induced current but not affecting any of our conclusions about its properties. In all voltage-ramp figures, the absolute zero current level is indicated by a thin continuous horizontal line.

(2) As already mentioned, in many experiments we recorded the development of the modulator-induced current while holding the membrane at a steady voltage, usually −30 mV (e.g., Fig. 1*B*).

(3) Finally, we used the voltage steps to characterize the voltage and time dependence of the modulator-induced current, as well as to check for possible effects of the modulators on other preexisting voltage-dependent currents (see Fig. 12 and Results).

Solutions, drugs, modulators. Normal artificial seawater (ASW), used in most of the experiments, contained (in mM) 460 Na^+, 10 K^+, 11 Ca^{2+}, 55 Mg^{2+}, 602 Cl^-, and 10 HEPES buffer (pH 7.6, in some experiments 6.6 or 8.6). Other solutions were made by equimolar substitution of this basic formula. Na^+ was completely replaced with Tris, *N*-methyl-D-glucamine, or bis-tris propane [giving the solutions referred to as "0Na(Tris) ASW," "0Na(NMDG) ASW," and "0Na(BTP) ASW"]. Ca^{2+} was completely replaced with Co^{2+} ("0Ca ASW"). K^+ was decreased to 2 mM or increased to 30, 50, or 100 mM in exchange for Na^+ ("2, 30, 50, 100K ASW"); 460 mM (76%) of the Cl^- was replaced with isethionate, D-gluconate, or methanesulfonate ["142Cl(isethionate, gluconate, methanesulfonate) ASW"]. Fifty or 460 mM tetraethylammonium was substituted for Na^+ ("50, 460TEA ASW"). Sometimes two of these substitutions were made simultaneously. Smaller amounts of ions and drugs (up to 30 mM) were added without substitution.

The drugs and modulators used in these experiments were as in the preceding article (Březina et al., 1994d), except that, in addition to $buccalin_A$, $buccalin_B$ (Vilim et al., unpublished observations) and $buccalin_C$ (Miller et al., 1993) were also tested. All drugs and modulators were applied by bath perfusion. When forskolin, 1,9-dideoxyforskolin, or Ro 20-1724 was used, the bath solution also contained up to 0.1% v/v of the stock solvent dimethyl sulfoxide (DMSO). In control experiments with standard voltage ramps between −100 and −30 mV, we found that as much as 0.5% DMSO alone had no obvious effect on the basal currents present in this voltage range, did not prevent activation of the modulator-induced current by 5-HT or MM_A (four fibers), and had no effect on that current when added after the current had already been activated (two fibers).

Results

The postsynaptic modulators induce outward current in the physiological operating voltage range of ARC muscle fibers

Physiologically, the nonspiking ARC muscle operates between a resting potential no more negative than −80 mV and a maximally ACh-depolarized potential no more positive than about −25 mV (Březina et al., 1994b). The steady state *I–V* relation of the basal, unmodulated currents present in this voltage range typically rectifies inwardly below about −70 mV and outwardly above about −50 or −40 mV, with a plateau region of high or even negative slope resistance between the two regions of rectification (e.g., Figs. 1*Ca*, 3*A*; Březina et al., 1994a).

When comparable steady state *I–V* relations were obtained in the presence of the SCPs, MMs, or 5-HT, it was apparent that all of these postsynaptic modulators (though not all equally; see below) induced an outward current in the physiological voltage range that grew larger with depolarization, becoming significant particularly over the plateau region and at more positive voltages (e.g., Fig. 1*Aa,Ab*). Such current was observed in nine fibers tested with SCP_A, 58 with SCP_B, 266 with MM_A, 17 with MM_B, and 175 with 5-HT. We generally studied the outward

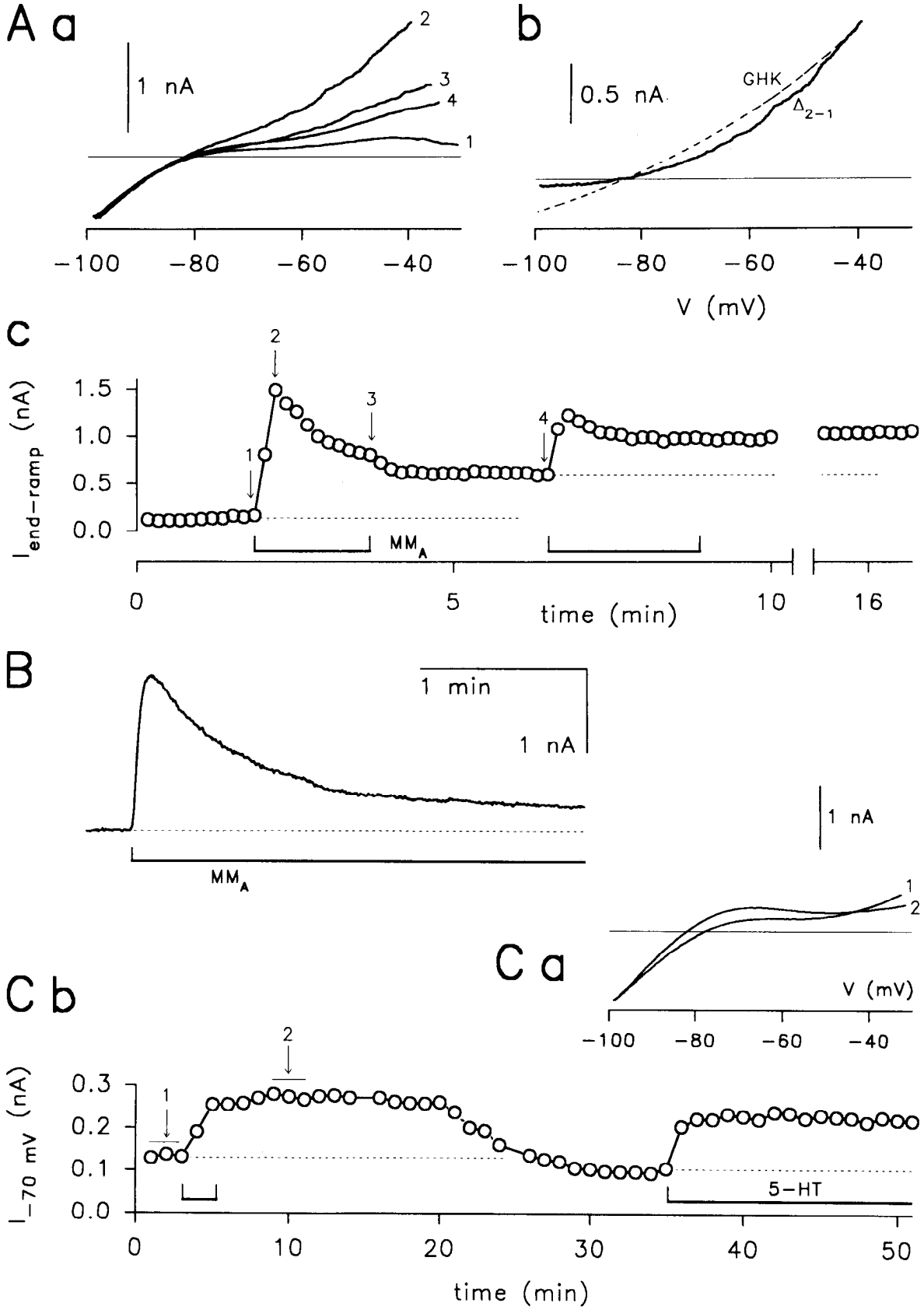

Figure 1. The postsynaptic modulators induce outward current in the physiological operating voltage range of ARC muscle fibers. Steady state *I–V* relations were obtained with standard slow (14 mV/sec) voltage ramps between nominally −100 and −30 mV every 10 sec (*A*) or 60 sec (*C*), or the fiber was held steady at −30 mV and the holding current monitored (*B*), all in normal ASW (see Materials and Methods). *A*, Effect of two applications of 1 μM MM_A. *Ac* is a plot of values of the absolute current measured at the end (the most positive voltage reached) of successive ramps; *Aa* shows the complete *I–V* relations obtained at the times indicated in *Ac*. *Ab* shows the difference *I–V* relation of net MM_A-induced current

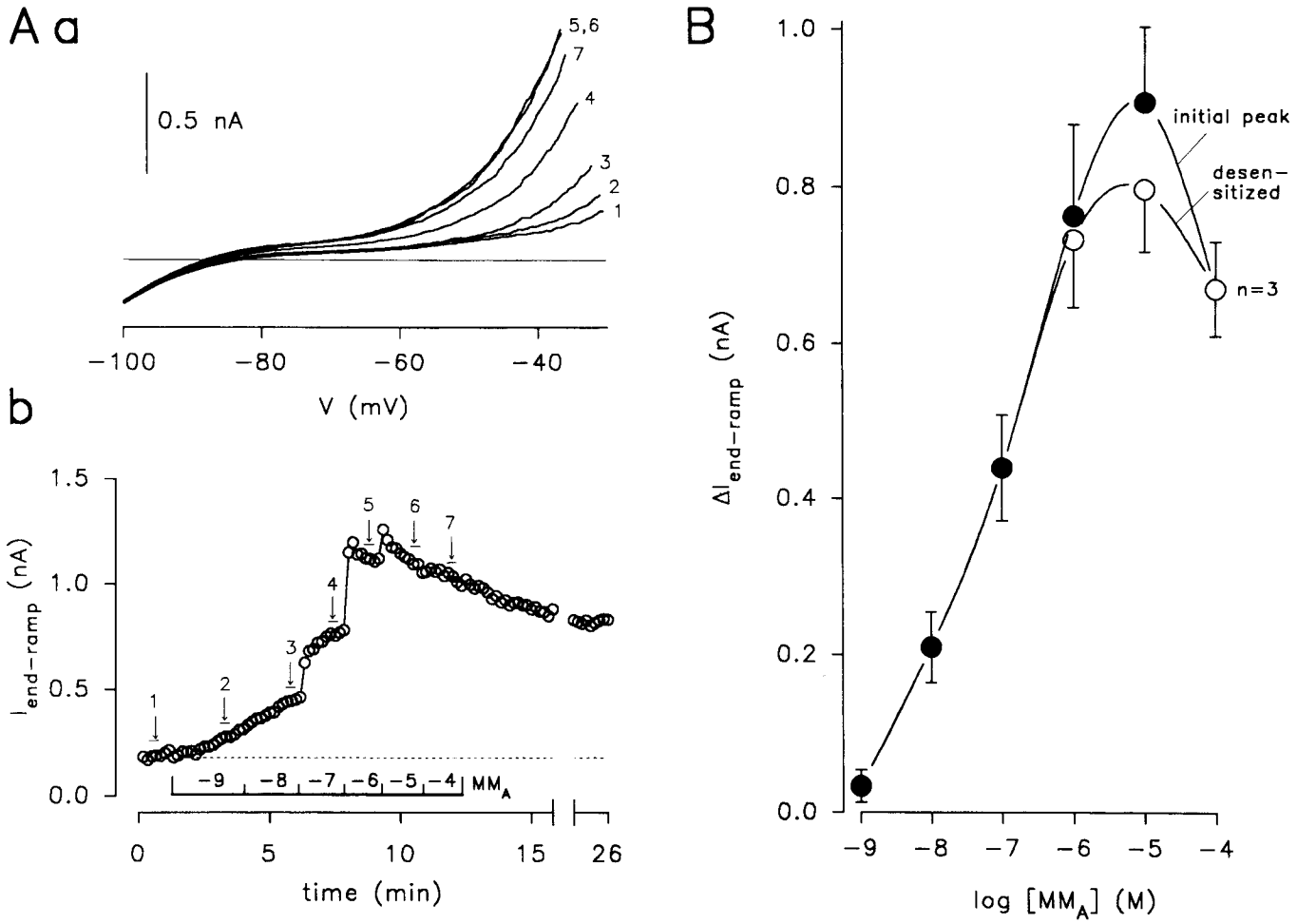

Figure 2. MM_A activates a large outward current: dose–response relation. *A, I–V* relations were obtained with standard voltage ramps every 10 sec in normal ASW while successively higher concentrations of MM_A, from 1 nM to 100 μM (10^{-9} to 10^{-4} M), were applied. *Ab* is a plot of values of the absolute current measured at the end (the most positive voltage reached) of successive ramps; *Aa* shows the complete *I–V* relations (each an average of three consecutive relations) obtained at the times indicated in *Ab*. The fiber was exposed to each MM_A concentration only briefly (for 1–3 min), probably leading to an underestimate of the slowly developing effect of the lower concentrations. The effect of high MM_A concentrations was most likely also underestimated (see *B*), because of gradual desensitization within this cumulative-application paradigm necessitated by the long persistence of the outward-current response (see text). *B,* Summary dose–response plot (means ± SEMs) of values from *Ab* and two other fibers of the amplitude of outward current, measured at the end of the voltage ramp, activated by different MM_A concentrations. For the higher concentrations, both the peak current activated immediately upon application and the steady state current after desensitization are plotted; the apparent decrease in efficacy at 10^{-4} M MM_A is most likely an artifact of prior desensitization by the lower concentrations applied earlier.

current at voltages negative to −30 mV in part so as to avoid its contamination by the inward current arising from the simultaneous enhancement by the modulators of the Ca current, which becomes significant positive to −30 mV (Březina et al., 1994d). Nevertheless, in a small percentage of fibers (e.g., Fig. 1*Ca*) we observed an inward current shift superimposed on the modulator-induced outward current already somewhat negative of −30 mV, which may have been due to the Ca-current enhancement.

The concentrations required to activate the outward current were quite similar for all of the postsynaptic modulators—MM_A (Fig. 2; complete dose–response relations between 1 nM and 100 μM were obtained in three fibers), MM_B (Fig. 3*C*, three fibers), 5-HT (Fig. 3*B,C*, seven fibers), and SCP_A and SCP_B (Fig. 3*C*, three and five fibers, respectively). All began to activate noticeable outward current around 10 nM, and had maximal effects above 10 μM. It was difficult to determine the saturating concentrations precisely (see particularly Fig. 2) because the modulator-induced outward current did not easily wash out, so that complete dose–response relations within the same fiber could

←

obtained by subtracting *trace 1* from *trace 2* in *Aa* (*solid line*), compared with K current predicted by the Goldman-Hodgkin-Katz constant-field equation (*dashed line*) using extracellular and intracellular K^+-concentration values, 10 and 260 mM, that give the observed reversal potential, and an arbitrary total permeability. *B,* Outward current induced by 10 μM MM_A at a steady holding potential of −30 mV. *C,* Effect of two applications of 1 μM 5-HT. *Cb* is a plot of values of the absolute current measured at −70 mV (the approximate voltage where the outward current induced by 5-HT was largest in this particular fiber); *Ca* shows the complete *I–V* relations (each constructed from averages of three consecutive pairs of raw current and voltage traces) obtained at the times indicated in *Cb*. Note the inward current shift superimposed on the 5-HT–induced outward current at the more positive voltages (see text).

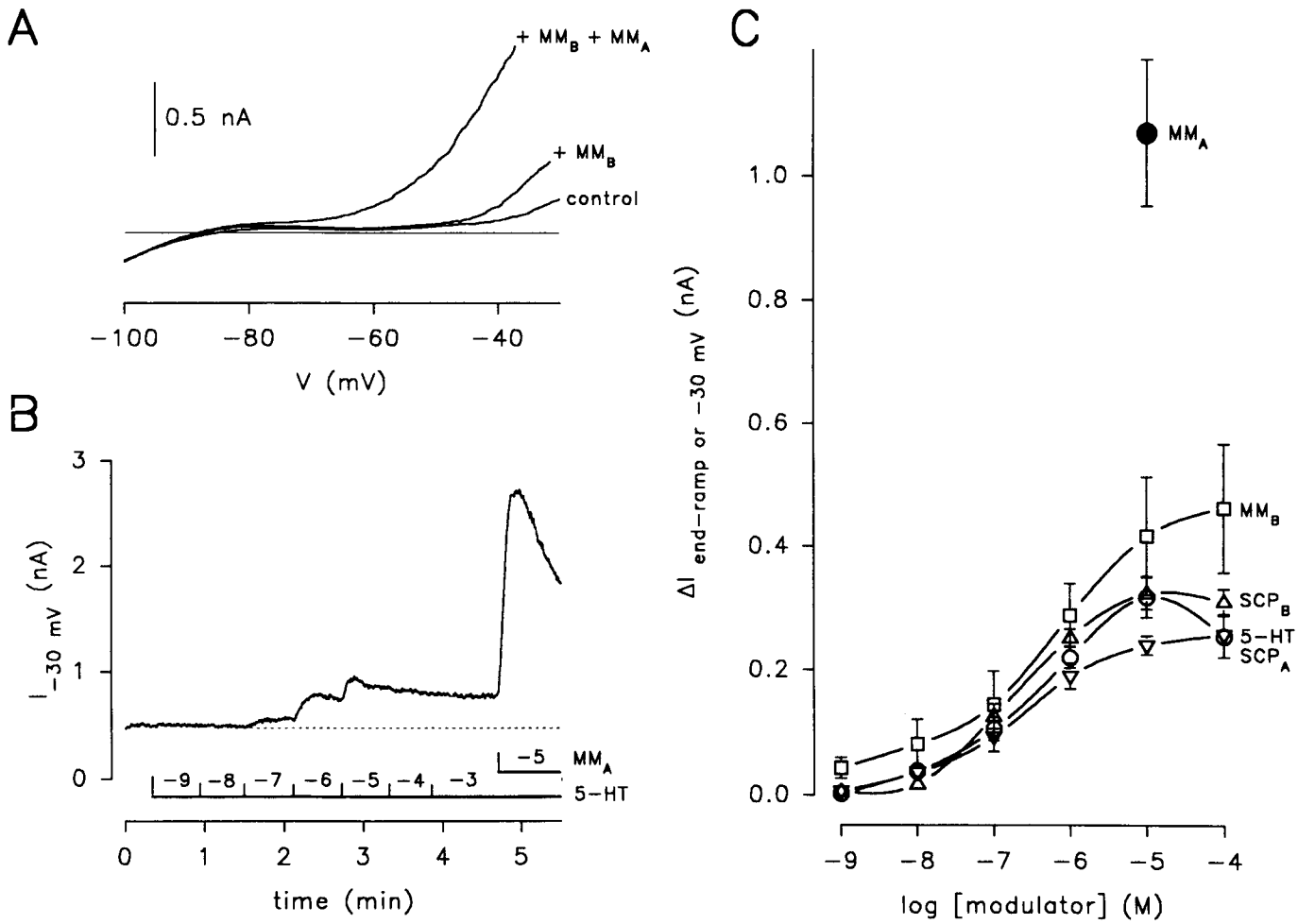

Figure 3. MM_B, SCP_A, SCP_B, and 5-HT activate small outward currents: dose–response relations. *A*, *I–V* relations obtained with standard voltage ramps first in control normal ASW, then after application of 100 μM MM_B, and finally after further application of 100 μM MM_A. *B*, Continuous record of the holding current at −30 mV in normal ASW while successively higher concentrations of 5-HT, from 1 nM to 1 mM (10^{-9} to 10^{-3} M), were applied, followed by further final addition of 10^{-5} M MM_A to the solution still containing 10^{-3} M 5-HT. *C*, Summary dose–response plots (means ± SEMs) of the amplitude of outward current activated by different MM_B, SCP_A, SCP_B, and 5-HT concentrations. The MM_B plot is derived from three experiments carried out as in Figure 2*A*; plotted are increases in outward current at the end of the voltage ramp (the most positive voltage reached). The 5-HT plot is derived from the experiment in *B* and six others (including two in which only part of the series of measurements could be completed); plotted are peak increases in outward current at −30 mV. The SCP_A plot is derived from three similar experiments, and the SCP_B plot from five similar experiments (including one in which only part of the series of measurements could be completed). At the end of all three experiments with MM_B, six with 5-HT, and two each with SCP_A and SCP_B (thus $n = 13$), 10 or (in the experiments with MM_B) 100 μM MM_A was added to the solution still containing the highest concentration of the other modulator; the amplitude of the additional large outward current activated by MM_A is plotted.

only be obtained by cumulative application of successively higher concentrations of the modulators, but the larger currents activated by the higher modulator concentrations desensitized (see below). Nevertheless, increasing the modulator concentrations beyond 10 μM generally did not activate significant additional outward current in the cumulative applications (Figs. 2*Ab*, 3*B*), and it was our impression from several experiments that the same would have been found if the effects of single high concentrations were compared statistically between fibers.

There was, however, a major difference in the maximal amplitude of outward current that the different modulators were able to activate. MM_A activated large outward currents, with peak amplitudes (before desensitization) often around 1 nA but sometimes up to 3 nA at −30 mV (e.g., Figs. 1*A,B*; 2; 3*C*). In contrast, even saturating concentrations of all of the other postsynaptic modulators—5-HT, SCP_A, SCP_B, and, interestingly, the other MM studied, MM_B—activated outward currents generally no larger than 0.3–0.5 nA at −30 mV, two or three times smaller than the MM_A-induced current (Figs. 1*C*, 3). (Occasionally, however, somewhat larger currents, up to 0.8 nA, were activated in particular by 5-HT; see, e.g., Fig. 13*B*.) As a result, when a saturating concentration of one of these modulators had activated its maximal activatable current, judging by the fact that higher concentrations had no greater effect, further addition of MM_A was still able to induce substantial additional outward current (Fig. 3; >150 fibers, since we routinely added MM_A at the end of most experiments with the other modulators). Apart from the difference in maximal amplitude, the outward currents activated by MM_A and the other modulators appeared to differ somewhat also in their voltage dependence (see next section).

Upon application of the higher concentrations of the modulators, the outward current developed within a few seconds (e.g., Fig. 1*B*); however, this rate was almost certainly limited by the speed of bath perfusion (see Materials and Methods of Březina

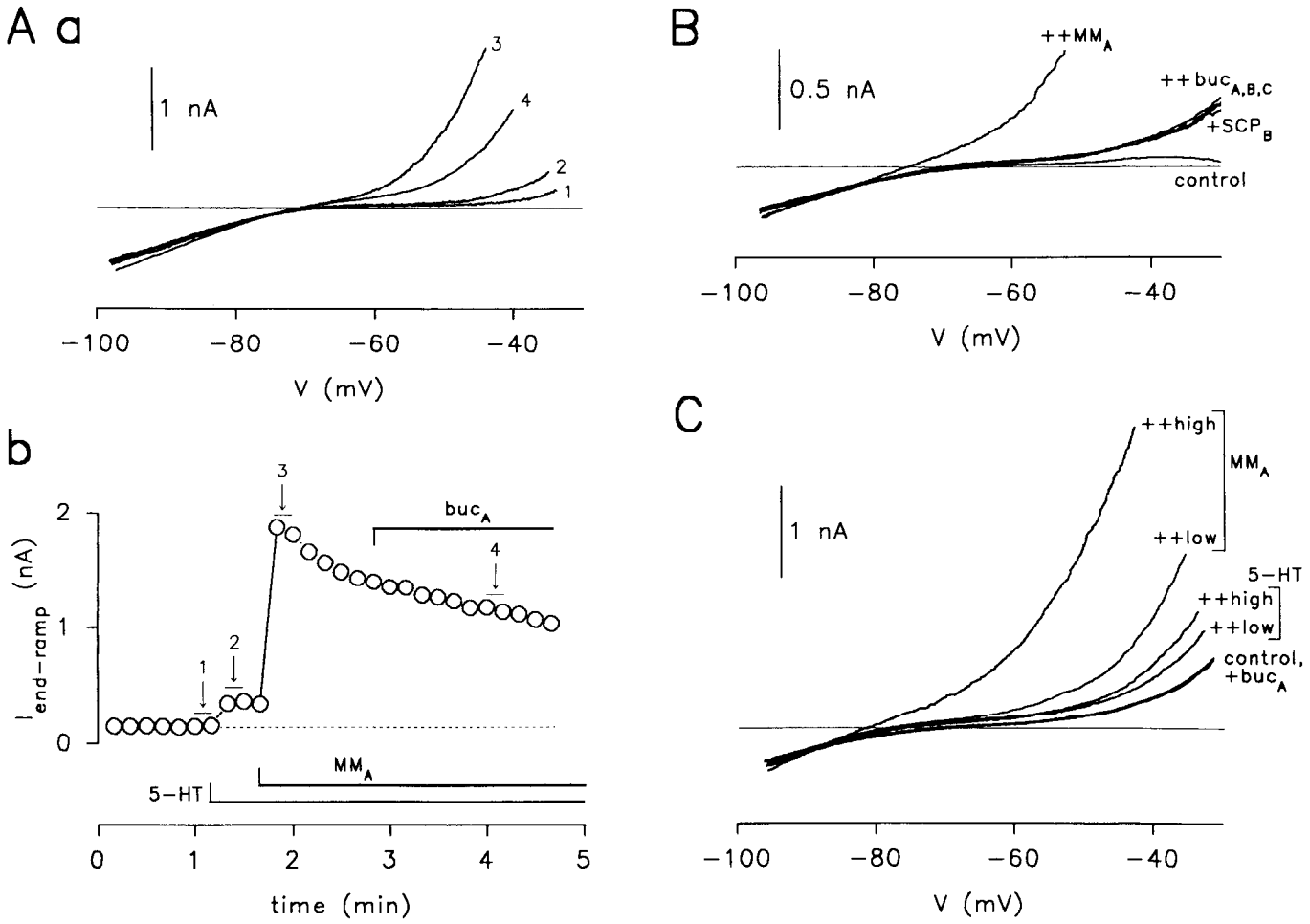

Figure 4. Buccalins do not activate any outward current, and have no effect on the outward-current responses to the postsynaptic modulators. *I–V* relations were obtained with standard voltage ramps in normal ASW. *A*, Buccalin$_A$ has no effect on outward current already activated by 5-HT and MM$_A$. *Ab* is a plot of values of the absolute current measured at the end (the most positive voltage reached) of successive ramps; *Aa* shows the complete *I–V* relations (each an average of two consecutive relations) obtained at the times indicated in *Ab*. All of the modulators were applied at 10 μM. *B*, Buccalins$_{A,B,C}$ have no effect on the small outward current already activated by SCP$_B$, and their presence does not prevent or apparently reduce the usual additional large response to MM$_A$. All of the modulators were applied at 10 μM. The ++*MM$_A$* *I–V* relation has been clipped at the top edge of the panel. *C*, When applied first, buccalin$_A$ does not activate any outward current, and its presence does not prevent or apparently alter the dose–response characteristics (compare Figs. 2, 3*B,C*) of the small outward-current response to 5-HT or the further large response to MM$_A$. All of the modulators were added cumulatively, without washing out the modulators already present, in the following order: 10 μM buccalin$_A$, 500 nM (*low*) 5-HT, 10 μM (*high*) 5-HT, 50 nM (*low*) MM$_A$, and 10 μM (*high*) MM$_A$. The low and high concentrations of 5-HT and MM$_A$ were chosen from the dose–response relations in Figures 3*C* and 2*B* to give, respectively, clearly visible but submaximal, and maximal activation of outward current.

et al., 1994a,d). With low modulator concentrations, the current often developed distinctly more slowly (e.g., Fig. 2*Ab*). In the continued presence of the modulators, the current desensitized, over several minutes, to a final steady state current that often amounted to 30–50% of the initial peak current. The rate and extent of the desensitization increased with the modulator concentration applied; concentrations below 1 μM usually gave little desensitization. However, the desensitization seemed to depend also on the amplitude of the current. Thus, the large MM$_A$-induced currents almost invariably desensitized strongly (e.g., Fig. 1*Ac,B*), while the smaller currents activated by even high concentrations of the SCPs, 5-HT, or MM$_B$ desensitized much less (Figs. 1*Cb*, 3*B*). However, when on occasion these modulators activated unusually large currents, these also desensitized considerably (e.g., Fig. 13*B*).

Like the Ca-current effect of the modulators (Březina et al., 1994d), the modulator-induced outward current persisted for a long time after the end of the modulator application. Part of the large MM$_A$-induced current sometimes washed out within several minutes, but the bulk of the current, and those activated by the other modulators, persisted often for 20 min or longer (Figs. 1*Ac,Cb*; 2*Ab*; see Fig. 8*C*). The desensitization also persisted: although occasionally it was possible, after a prolonged wash, to obtain a second response of the same amplitude as the first (Fig. 1*Cb*), more often the second response was considerably smaller even after a wash as long as 30 min (Fig. 1*Ac*; see Fig. 13*B*). Interestingly, in acidified solution or Ca^{2+}-free, Co^{2+}-containing solution, the modulator-induced outward current appeared to wash out much faster (see later).

In contrast to the postsynaptic modulators, the buccalins, which are thought to act presynaptically on the ARC-muscle motor neurons and not directly on the muscle itself (Cropper et al., 1988, 1990), did not activate any outward current between −100 and −30 mV at any concentration between 10 nM and

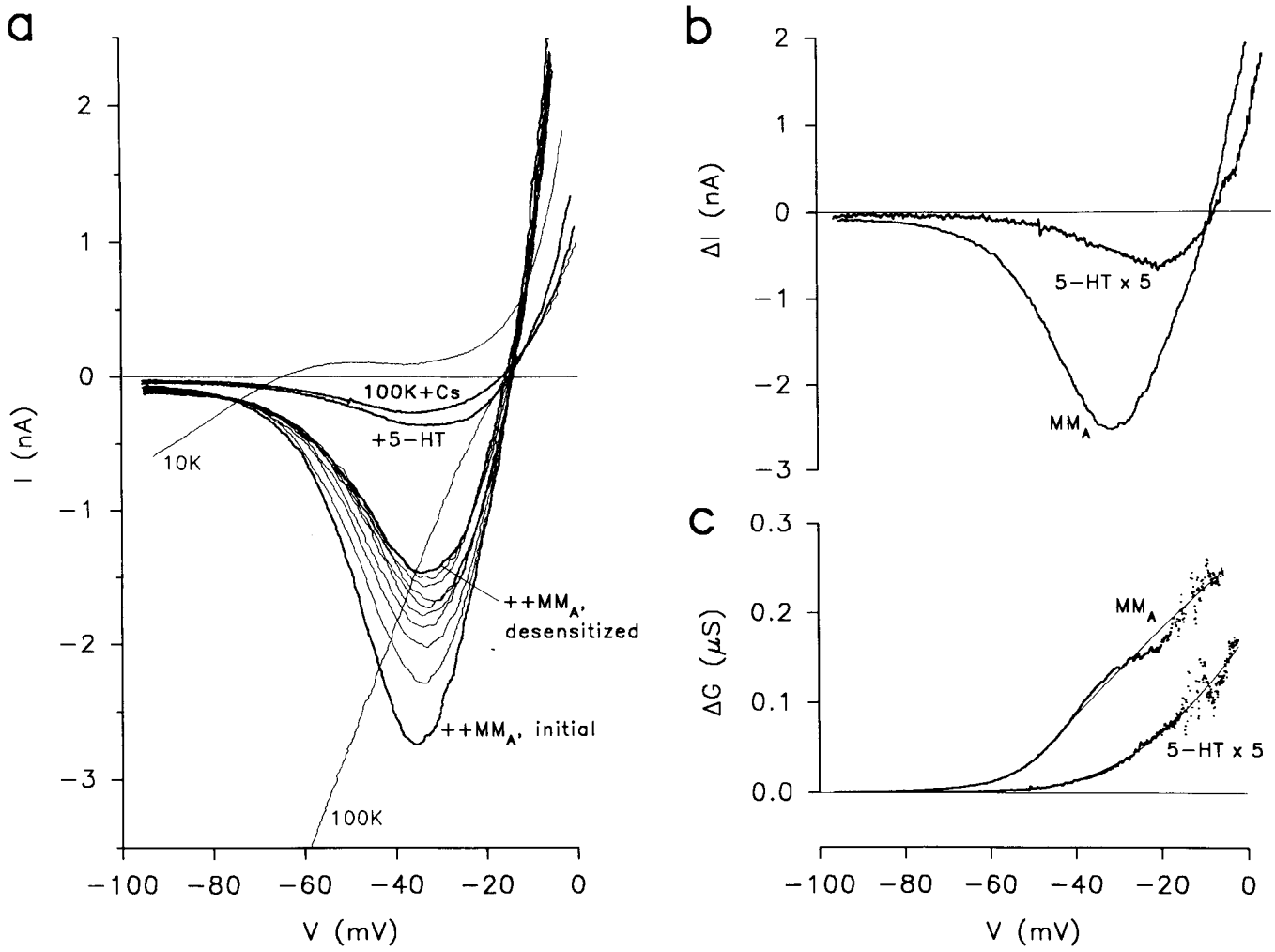

Figure 5. The modulator-induced outward current is a voltage-dependent K current. The *I–V* relations shown in *a* were obtained with slow (14 mV/sec) voltage ramps from nominally −100 to 0 mV, in the following order: *10K* (normal ASW), *100K* (100K ASW), *100K + Cs* (after addition of 30 mM Cs^+ to the 100K ASW), *+ 5-HT* (after further addition of 10 μM 5-HT), and finally the *++MM_A* relations (after further addition of 10 μM MM_A; the relations shown were obtained at 10 sec intervals as the MM_A-induced current desensitized). Note that the effect of the modulators is truly due to activation of the K current rather than enhancement of the Ca current: the Ca current is seen at considerably more positive potentials (e.g., Fig. 4*B* of Březina et al., 1994d), and in any case is not seen at all with slow voltage ramps except when masking K currents are blocked (e.g., Fig. 1*A* of Březina et al., 1994b). *b,* Difference *I–V* relations of the net 5-HT- and MM_A-induced currents, obtained by subtracting the *+5-HT* and *++MM_A, initial I–V* relations from the *100 K + Cs* relation in *a.* The 5-HT–induced current has been scaled up fivefold for clarity. Note the voltage dependence and the shifted reversal potentials of both the 5-HT- and MM_A-induced currents. *c, G–V* plots of the 5-HT- and MM_A-activated (chord) conductance, obtained by dividing the difference currents in *b* by the apparent driving force. Cs^+ was included in this and most similar experiments with high-K^+ ASW (e.g., Fig. 6*B*) in order to block the inwardly rectifying K current, the major current dominating the hyperpolarized voltage range studied (Březina et al., 1994a). As seen in *a,* this current became very large in high-K^+ ASW and, if left unblocked, would have made accurate measurement of the smaller modulator-induced currents difficult. In normal ASW, even 30 mM Cs^+ did not appear to affect the modulator-induced outward current significantly, at least at the more positive voltages where the current was prominent (see Fig. 9*A* and text). However, it was possible that Cs^+ nevertheless blocked the current to some extent, like the inward rectifier, in a voltage-dependent manner, at the more negative voltages. Such block might not have been evident in normal ASW, but would have become more apparent as the inward modulator-induced current at negative voltages increased in the high-K^+ ASW. Indeed, the turnoff of the current with hyperpolarization seemed somewhat sharper in high-K^+ ASW containing Cs^+ than in the few experiments done without Cs^+ (compare, e.g., Fig. 6*A,B*). Thus, although the intrinsic voltage dependence of the modulator-induced current was clearly considerable, it may have been somewhat exaggerated here and in Figure 6*B* by a weak voltage-dependent block of the current by Cs^+.

100 μM (Fig. 4*C*). Eleven fibers were tested with $buccalin_A$, and four with $buccalin_B$ (Vilim et al., unpublished observations) and $buccalin_C$ (Miller et al., 1993). In the presence of even 10 μM of the buccalins, all of the postsynaptic modulators were still able to activate, with about the usual potency (Fig. 4*C*), outward currents of normal amplitude and *I–V* characteristics (Fig. 4*B,C*). Finally, addition of 10 μM $buccalins_{A,B,C}$ had no effect on outward currents already activated by maximal (10 μM) or submaximal (50–500 nM) concentrations of MM_A, 5-HT, or SCP_B (Fig. 4*A,B*, nine fibers). In the preceding article, we similarly found that at least $buccalin_A$ did not affect the Ca current in the ARC muscle fibers or its enhancement by the postsynaptic modulators (Březina et al., 1994d).

The modulator-induced outward current is a voltage-dependent K current

The modulator-induced outward current was (as described further below) strongly voltage dependent, enhanced by depolar-

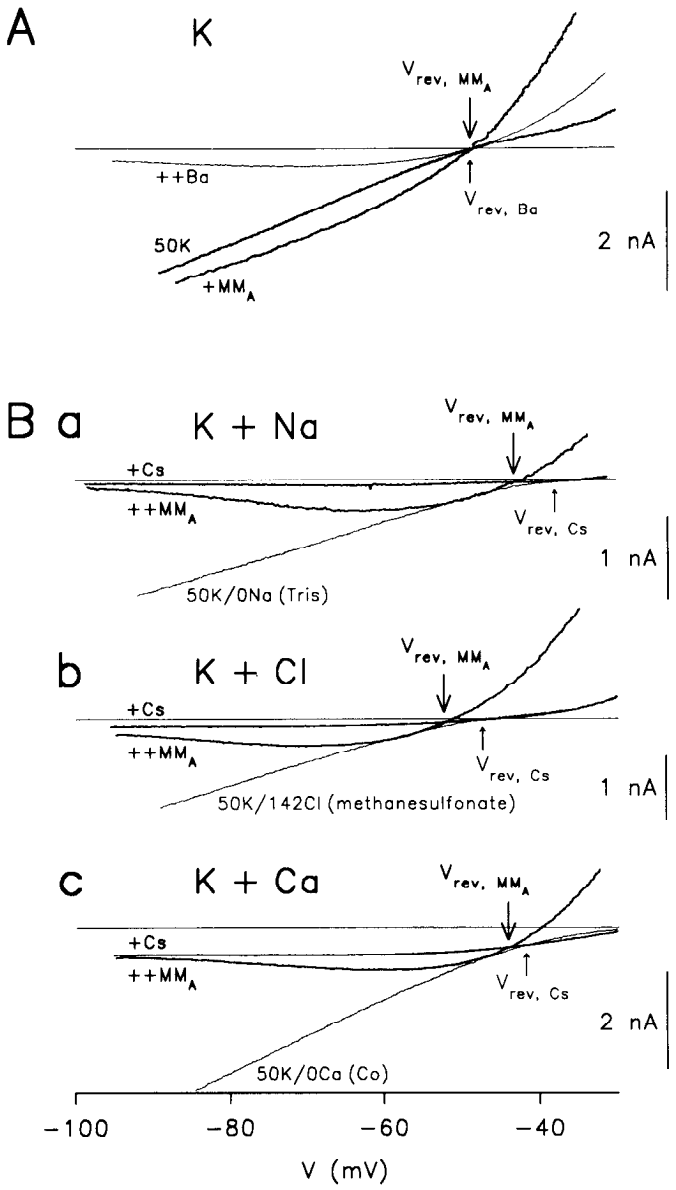

Figure 6. The reversal potential of the modulator-induced outward current shifts with altered extracellular K^+ but not Na^+, Cl^-, or Ca^{2+}. *A*, Alteration in extracellular K^+ only. *I–V* relations were obtained with standard ramps first in control 50K ASW, then following application of 10 μM MM_A, and finally after further addition of 5 mM Ba^{2+}. *B*, Alteration in extracellular Na^+, Cl^-, or Ca^{2+} as well as K^+. These experiments were carried out as in *A*, except that, in the 50K ASW, all extracellular Na^+ was additionally replaced with Tris (*Ba*), or 460 mM (76%) of the extracellular Cl^- was replaced with methanesulfonate (*Bb*), or all extracellular Ca^{2+} was replaced with Co^{2+} (*Bc*). Furthermore, 30 mM Cs^+ was applied instead of Ba^{2+}, before the 10 μM MM_A rather than after it. The alterations in Na^+, Cl^-, and Ca^{2+} were carried out in the 50K ASW rather than normal ASW because the elevated K^+ shifted the reversal potential of the modulator-induced current to more positive voltages where the current was more activated, making evaluation of the reversal potential, and any further shifts in it in response to the altered Na^+, Cl^-, or Ca^{2+}, considerably easier. Note that, in all of the solutions tested, the reversal potential of the MM_A-induced current, V_{rev,MM_a}, always approximates E_K, as estimated by the reversal potential of the Ba^{2+} or Cs^+ block of the inwardly rectifying K current, $V_{rev,Ba/Cs}$ (the Cs^+ reversal potential was consistently several millivolts more positive than the MM_A reversal potential, perhaps due to the secondary outward current shift that Cs^+ begins to induce at these relatively depolarized voltages; see, e.g., Fig. 9*A*, and Březina et al., 1994a). Furthermore, the MM_A reversal potential is not changed significantly by the altered Na^+, Cl^-, or Ca^{2+}. (The differences in MM_A reversal potential between the four fibers shown here were not due to any systematic solution dependence, but simply interfiber variability. Variations just as large were observed between different fibers in the same solution; note that $V_{rev,Cs}$—i.e., E_K—varies in parallel with V_{rev,MM_a}.)

ization, and turned off by hyperpolarization. With hyperpolarization, the small currents activated by the SCPs, 5-HT, and MM_B usually became too small to be resolvable at voltages more negative than about −60 or −70 mV; thus, any reversal potential could not be clearly distinguished. MM_A-induced currents, on the other hand, were large enough that, though they likewise turned off with hyperpolarization, they could be followed often down to at least −100 mV. Clear reversals of the MM_A-induced current were then often evident (e.g., Fig. 4*Aa,B*; see Fig. 7*Aa*). In normal (10 mM K^+) ASW, the current typically became inward below about −80 mV, close to the estimated value of the K^+ equilibrium potential, E_K, in this solution (Březina et al., 1994a). Thus, it seemed likely that at least the MM_A-induced current was carried principally by K^+. [In some experiments it appeared that the modulator-induced current remained outward at voltages much more negative than any reasonable value of E_K (e.g., Figs. 1*Ca*, 2*Aa*). This may have been due to a gradual, modulator-independent outward shift of the whole *I–V* relation that we sometimes saw progressively develop during the experiment. The *I–V* relations before and after the modulator application were obtained tens of seconds or minutes apart; since the two relations typically crossed at a shallow angle, even a very small outward shift during this interval would have offset the apparent reversal potential negative by many millivolts.]

To confirm the K^+ dependence of the modulator-induced current, we elevated the extracellular K^+ concentration from the normal 10 mM to 30, 50, or 100 mM. As expected, the MM_A-induced current now reversed considerably more positive, in a voltage range where the current's voltage dependence (which apparently remained unchanged; see below) made it much larger so that the reversal potential could be determined much more accurately. Furthermore, for the same reason, clear reversal potentials of the small currents activated by SCP_B and 5-HT could now be distinguished, invariably very close to, and not obviously systematically different from, the MM_A reversal potential (e.g., Fig. 5*a,b*). In 18 fibers in 50K ASW, MM_A-, SCP_B-, and 5-HT-induced currents reversed at −44 ± 1.4 mV (mean ± SEM; Fig. 6*A*). In 100K ASW, the currents reversed often between −30 and −20 mV, in some fibers even more positive (Fig. 5*a,b*, 11 fibers). These shifts in reversal potential closely approximated those predicted by the Nernst equation for a K^+-selective conductance: if E_K was about −80 mV in normal 10K ASW (cf. Březina et al., 1994a), it should have shifted to about −40 mV in 50K and −22 mV in 100K ASW. It was possible to roughly monitor the actual shifts in E_K by the reversal potential of a bona fide K current, the inwardly rectifying K current prominent in the hyperpolarized portion of the basal as well as the modulated standard ramp *I–V* relations, visualized by its block by 1–5 mM Ba^{2+} or 30 mM Cs^+ (see Březina et al., 1994a, and Figs. 5, 6). The Ba^{2+}- or Cs^+-blocked inward rectifier indeed usually reversed not far from the modulator-induced currents, and both reversal potentials varied in parallel as the extracellular K^+ concentration was altered (Fig. 6). In contrast, neither reversal potential changed significantly when extracellular Na^+ was replaced with Tris, Cl^- with methanesulfonate or isethionate, or Ca^{2+} with Co^{2+}. When these substitutions were made in

←

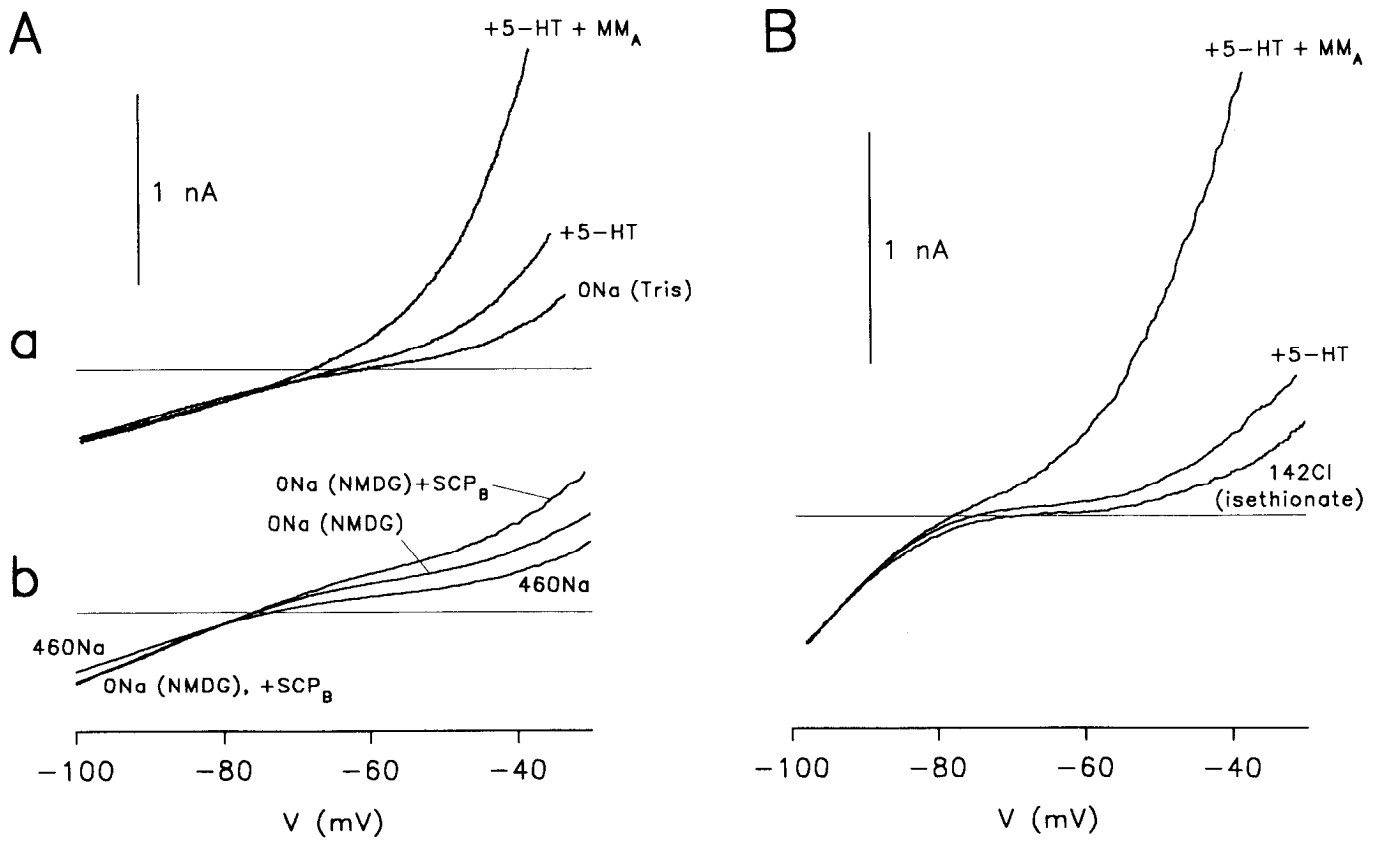

Figure 7. The *I–V* characteristics and amplitude of the modulator-induced K current are not Na^+ or Cl^- dependent. *I–V* relations were obtained with standard voltage ramps. *Aa,* Normal K currents are activated by 10 μM 5-HT followed by 10 μM MM_A in 0Na(Tris) ASW. *Ab,* SCP_B at 1 μM activates normal K current in 0Na(NMDG) ASW. Note that the 0Na(NMDG) ASW itself induces a K current (Březina et al., 1994a). However, the two K currents are most likely different: the SCP_B-induced current simply adds to the NMDG-induced current, and is not obviously occluded by it. Furthermore, the NMDG-induced current appears significantly less voltage dependent than the SCP_B-induced current: below E_K, the NMDG-induced current is clearly inward, that is, little or not at all turned off by hyperpolarization, whereas the SCP_B-induced current turns off completely. *B,* Normal K currents are activated by 10 μM 5-HT followed by 10 μM MM_A in 142Cl(isethionate) ASW.

the 50K ASW, the modulator-induced currents still reversed at −46 ± 1.5 mV (nine fibers; Fig. 6*B*; see also Figs. 7, 8, and next section). Taken together, these results argued strongly that the outward currents activated by MM_A, SCP_B, and 5-HT were all carried principally by K^+.

We have already mentioned the voltage dependence of the modulator-induced K current. Already in normal 10 mM K^+ ASW, the outward rectification of the current was considerably greater than predicted purely from the asymmetry between the intracellular and extracellular K^+ concentrations by the Goldman-Hodgkin-Katz constant-field equation (Fig. 1*Ab*). However, the voltage dependence became still more obvious when the extracellular K^+ concentration was elevated. The smaller disparity between the intracellular and extracellular K^+ concentrations, in addition to shifting the reversal potential positive, should have linearized the constant-field component of the current's rectification; a current that possessed no additional voltage dependence should then have been observed as a large inward current increasing steadily with hyperpolarization over the negative portion of the standard ramp-voltage range. Instead, the inward modulator-induced current below the reversal potential *decreased* dramatically as the membrane was progressively hyperpolarized to turn off almost completely, just as in normal ASW, around −100 mV (Figs. 5, 6*B*; but see Fig. 6*A* and Fig. 5 caption).

Interestingly, although both the large MM_A-induced current and the small MM_B-, SCP-, and 5-HT-induced currents showed qualitatively similar voltage dependence (e.g., Fig. 5*b*), it often appeared that the former began to activate with depolarization already somewhat negative of the latter, in both normal (e.g., Fig. 3*A*) and high-K^+ (Fig. 5*c*) ASW. Thus, a more negative voltage range of activation may have contributed to the larger size of the MM_A-induced current at any single potential within the physiological operating voltage range. (However, as described in the next section, the MM_A-induced current was also much larger even during steps to very positive voltages, and thus apparently absolutely larger.)

Further characteristics of the modulator-induced K current

Not just the reversal potentials, but also the *I–V* characteristics and typical amplitudes of the K currents activated by MM_A, SCP_B, and 5-HT were normal in ASW in which all Na^+ had been replaced with Tris (Fig. 7*Aa*, eight fibers), *N*-methyl-D-glucamine (NMDG; Fig. 7*Ab*, nine fibers), or bis-tris propane (nine fibers). Conversely, currents already activated by the modulators in normal ASW were not obviously affected by subsequent superfusion of these solutions (nine fibers). We previously reported that the NMDG-substituted solution itself activated a K current superficially not unlike the small modulator-induced currents (Březina et al., 1994a). However, the two K currents

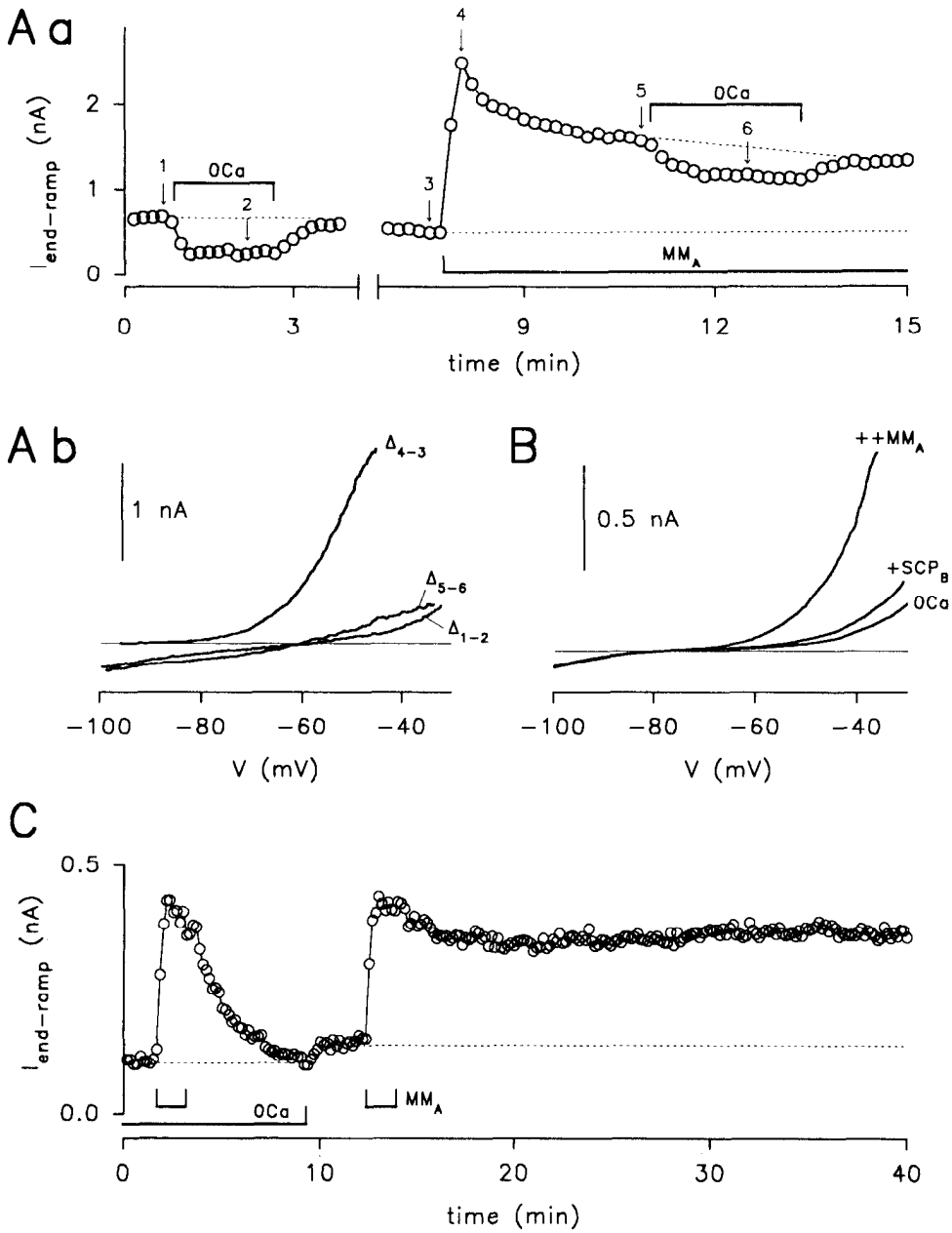

Figure 8. The modulator-induced K current is Ca^{2+} independent. *I–V* relations were obtained with standard voltage ramps. *Aa* is a plot of values of the absolute current at the end (the most positive voltage reached) of successive ramps; *Ab* shows the difference *I–V* relations obtained by subtracting the traces (themselves not shown) recorded at the times indicated in *Aa*. During the periods indicated, the normal ASW in the bath was replaced with 0Ca ASW, and 10 μM MM_A was applied. The difference *I–V* relation of Ca^{2+}-sensitive current (cf. Fig. 9*A* of Březina et al., 1994a) is similar whether obtained before (*trace 2* subtracted from *trace 1*) or after (*trace 6* from *trace 5*) development of the large MM_A-induced K current, and quite different from the *I–V* relation of the MM_A-induced current itself (*trace 3* from *trace 4*), which is therefore Ca^{2+} insensitive. *B*, Normal K currents are activated by 1 μM SCP_B followed by 1 μM MM_A in 0Ca ASW. *C*, Plot of values of absolute end-ramp current as in *Aa*, first in 0Ca ASW and then in normal ASW, in each of which 10 μM MM_A was applied briefly. In contrast to the usual resistance to washout of the MM_A-induced current in the normal ASW, in the 0Ca ASW the current washes out rapidly and completely once the MM_A application is terminated.

were most likely different. Their activation appeared to be mutually independent, without any obvious occlusion: even after the NMDG-induced current had developed, MM_A, SCP_B, and 5-HT were still able to activate currents of normal amplitude (Fig. 7*Ab*, nine fibers), and vice versa (five fibers). Furthermore, the NMDG-induced current appeared to be significantly less voltage dependent than the modulator-induced current (Fig 7*Ab*).

Similarly, all characteristics of the K currents activated by MM_A, SCP_B, and 5-HT appeared normal in ASW in which 76% of the Cl^- had been replaced with isethionate (Fig. 7*B*, three fibers), methanesulfonate (12 fibers), or D-gluconate (four fibers).

The modulator-induced K current was Ca^{2+} independent. The reversal potentials, *I–V* characteristics, and typical amplitudes of the currents activated by MM_A, SCP_B, and 5-HT were normal in ASW in which all Ca^{2+} had been replaced with Co^{2+} (0Ca ASW; Fig. 8*B*, 11 fibers). Currents already activated by MM_A in normal ASW were unaffected by subsequent superfusion of 0Ca ASW (Fig. 8*A*, two fibers). However, we did observe one clear effect of the Ca^{2+}-free solution: in it, the MM_A-, SCP_B-, and 5-HT-induced currents all washed out rapidly and completely once the modulator application was terminated, quite unlike their typical persistence in normal ASW (Fig. 8*C*, five fibers).

The K currents activated by MM_A, SCP_B, and 5-HT appeared normal in ASW alkalinized from the normal pH 7.6 to 8.6 (three fibers). They were also normal in most respects, though perhaps smaller than usual, in ASW acidified to pH 6.6 (eight fibers). However, in this solution, as in the 0Ca ASW, at least the MM_A-induced current washed out rapidly (four fibers).

Extracellular Cs^+ did not appear to block the K currents activated by MM_A, SCP_B, and 5-HT in any obvious way even at 30 mM (but see Fig. 5 caption), whether in normal 10K, 50K, or 100K ASW (Figs. 9*A*, 6*B*, 5*a*, respectively; 12 fibers). Currents

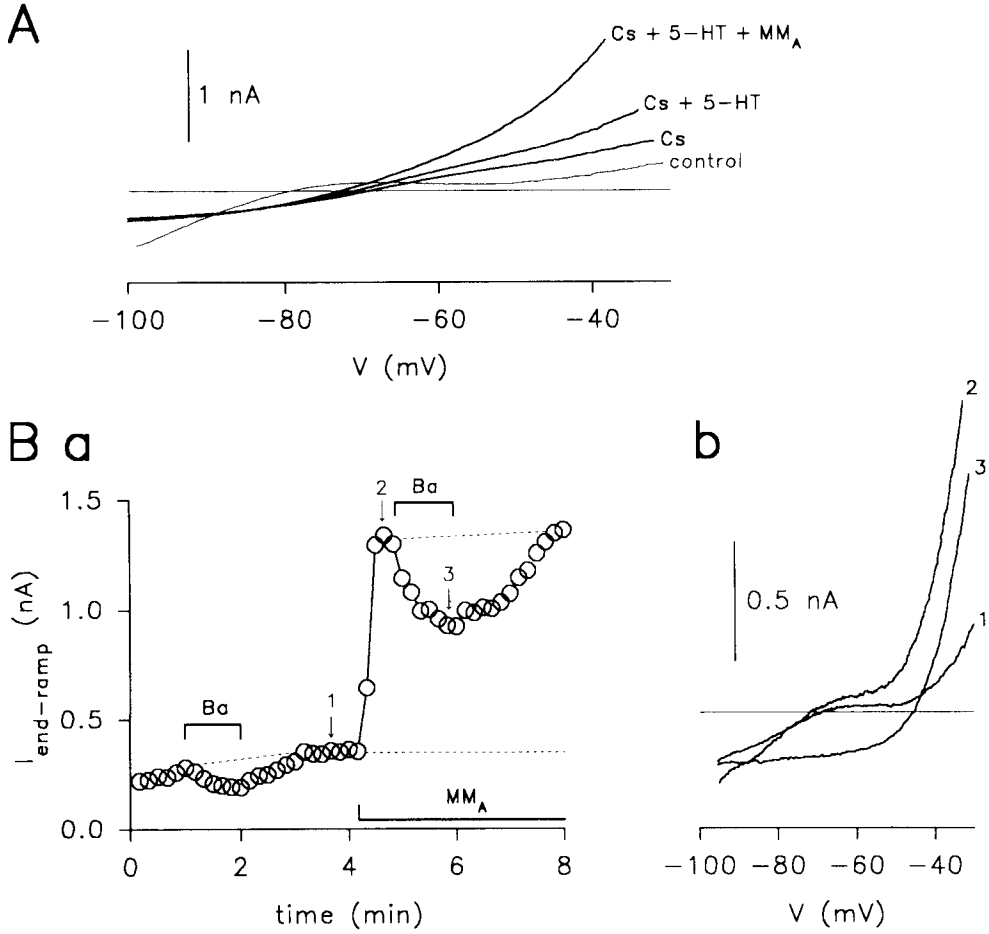

Figure 9. The modulator-induced K current is not readily blocked by extracellular Cs^+ or Ba^{2+}. *A, I–V* relations were obtained with standard voltage ramps first in control normal ASW and then following cumulative addition of 30 mM Cs^+, 10 μM 5-HT, and finally 10 μM MM_A. Both modulators activate apparently normal K currents in the Cs^+-containing solution. *B,* Effect of Ba^{2+}. *Ba* is a plot of values of the absolute current at the end (the most positive voltage reached) of successive standard voltage ramps in normal ASW; *Bb* shows the complete *I–V* relations obtained at the times indicated in *Ba.* During the periods indicated, 10 mM Ba^{2+} and 10 μM MM_A were added to the bath solution. The Ba^{2+}-induced inward current shift is larger after development of the MM_A-induced K current, potentially due to block of the current by the Ba^{2+}. However, 70% or more of the current clearly remains unblocked. Furthermore, examination of the *I–V* relations in *Bb* suggests that much of the apparent block may in fact be attributable to a shift of the whole *I–V* relation to more positive voltages (see text).

of roughly normal amplitude could be activated by the modulators also in the presence of as much as 10 mM Ba^{2+} (eight fibers). When Ba^{2+} was applied after the modulators had already activated the current, it had little effect on it at 1 or 3 mM, but at 10 mM induced (at −30 mV) an inward current shift that could be interpreted as partial (10–30%) block of the current (Fig. 9*Ba,* 10 fibers). However, comparison of complete *I–V* relations of the modulator-induced current before and after the Ba^{2+} application suggested that the apparent block was probably in large part simply a consequence of a shift of the whole *I–V* relation to more positive voltages (Fig. 9*Bb*), most likely due to increased screening of surface charge on the extracellular surface of the membrane by the added Ba^{2+}. Similar shifts upon alteration of extracellular divalent-cation concentrations are observed in the *I–V* relations of other currents in the ARC muscle fibers and many other preparations (Březina et al., 1994a,c).

Extracellular tetraethylammonium (TEA) blocked the modulator-induced K current, but only at high concentrations. Apparently normal-sized K currents were activated by MM_A, SCP_B, and 5-HT even in the presence of 50 mM TEA (Fig. 10*A*, five fibers); however, in 460 mM TEA the responses to the modulators were very small or absent (four fibers). Similar results were obtained when TEA was applied after the modulators had already activated the K current. TEA at 1–10 mM typically had no effect at all; 50 mM often induced some inward current shift at −30 mV, but generally no greater than could be accounted for by the effect of TEA on basal, modulator-independent currents (Fig. 10*B*; cf. Fig. 1*A* of Březina et al., 1994b); and only 460 mM substantially or completely blocked also the modulator-induced K current (Fig. 10*A,B*, 12 fibers).

In contrast, most of the modulator-induced K current was very potently blocked by the other traditional K-current blocker, 4-aminopyridine (4-AP). In many fibers, MM_A did not activate any K current at all in the presence of 10–100 μM 4-AP. However, we noted that in a significant number of fibers MM_A continued to activate *some* current (though no greater than 5% of the normal amplitude), and indeed continued to do so even in the presence of as much as 1–10 mM 4-AP (16 fibers). Similarly, the K-current responses to SCP_B and 5-HT appeared considerably reduced already in 10–100 μM 4-AP, but then persisted to some extent even in 10 mM 4-AP (four fibers). The *I–V* characteristics of the apparently 4-AP–resistant fraction were not obviously different from those of the whole modulator-induced K current. The absolute amplitudes of the 4-AP–resistant current activated by MM_A, SCP_B, and 5-HT were roughly comparable; though this was <5% of the normally large MM_A response, it was of course a considerably greater proportion, in some fibers perhaps as much as 50%, of the small responses to SCP_B and 5-HT. Similar results were obtained in the converse experiments in which 4-AP was applied after the modulators had already activated the K current. Block of the large MM_A-induced current was easily demonstrable. 4-AP at 10 μM typically blocked at least 80–90% of the current, 100 μM still more, and 1 mM usually had little or no further effect (Fig. 11*A,B*, 15 fibers). In some fibers, perhaps already 10 μM but certainly 100 μM 4-AP clearly blocked the whole MM_A-induced current at all

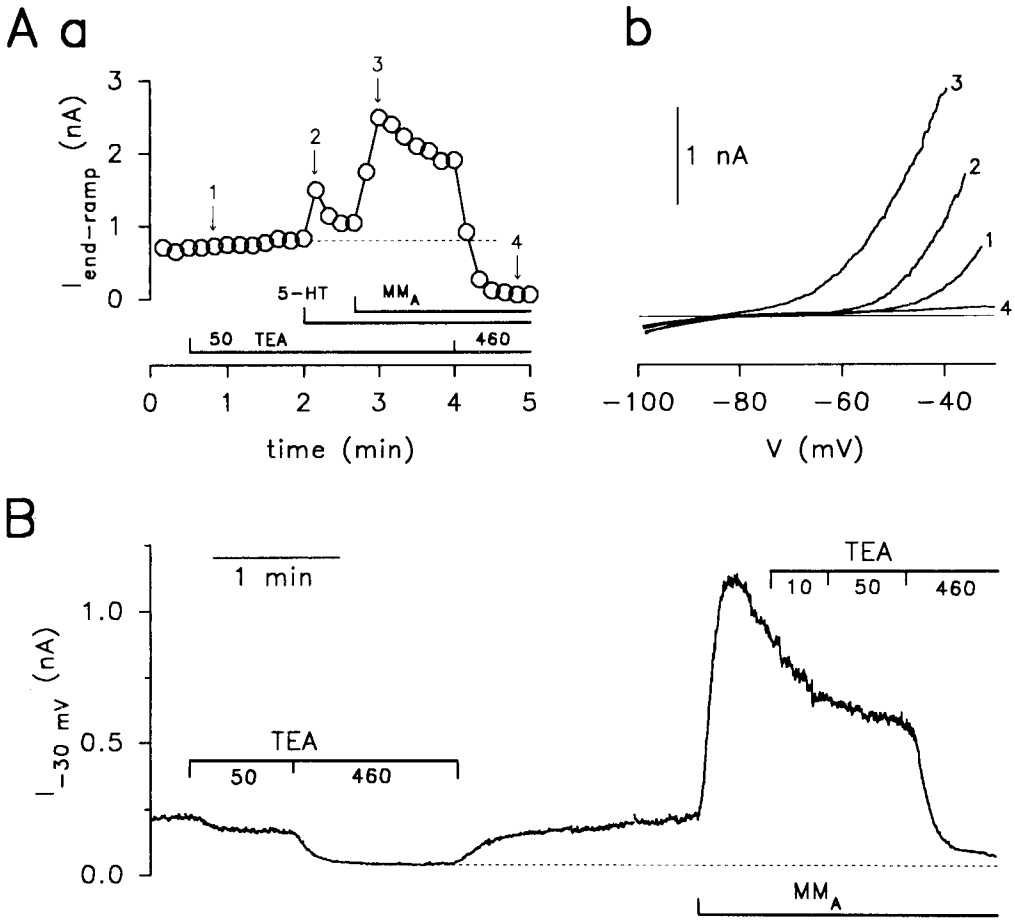

Figure 10. The modulator-induced K current is blocked only by high extracellular TEA. *A, I–V* relations were obtained with standard voltage ramps. *Aa* is a plot of values of the absolute current at the end (the most positive voltage reached) of successive ramps; *Ab* shows the complete *I–V* relations obtained at the times indicated in *Aa*. The experiment began in normal ASW, and continued in 50 and 460TEA ASW; 100 μM 5-HT and 10 μM MM_A were applied. Both modulators activate K currents of apparently normal amplitude and *I–V* characteristics even in the presence of 50 mM TEA; however, 460 mM TEA induces a large inward current shift, most likely by blocking the modulator-induced current as well as a component of modulator-independent current (see *B*). *B*, Continuous record of the holding current at a steady potential of −30 mV, during superfusion of 50 and 460TEA ASW before, and 10, 50, and 460TEA ASW after, activation of a large K current by 10 μM MM_A. The MM_A-induced current is clearly not significantly affected by 10 or even 50 mM TEA, but, together with a component of the modulator-independent holding current, is completely blocked by 460 mM TEA.

voltages between −100 and −30 mV (Fig. 11*A,B*) as well as at more positive voltages (see Fig. 12*A* and below). 4-AP block of the small SCP_B- and 5-HT-induced K currents was less dramatic and more variable from fiber to fiber (five fibers were tested with SCP_B, nine with 5-HT), as expected if indeed these currents included a larger, and variable, fraction of 4-AP–resistant current. In some fibers, practically the whole SCP_B- or 5-HT-induced current was clearly blocked by 10–100 μM 4-AP (Fig. 11*C*). In other fibers, however, even 1–10 mM appeared to have only a small effect (though there may have been appreciable error in separating the small current shifts due to activation of the modulator-induced current, its block by 4-AP, any small effect of 4-AP on basal currents, as well as any gradual modulator-independent alteration in the *I–V* relation during the experiment). Together, these results suggested the possibility that the total K current activated by each of the postsynaptic modulators perhaps included a small component of 4-AP–resistant current in addition to the larger current potently blocked by 4-AP.

Finally, we extended our examination of the modulator-induced K current beyond the standard ramp-voltage range by applying depolarizing steps to voltages as positive as +40 mV. We found, first, that the MM_A-induced current was much larger than the currents activated by SCP_B and 5-HT at these depolarized just as at the more hyperpolarized voltages (e.g., Fig. 12*Aa,Ab*), suggesting that it was larger not simply because its voltage range of activation was more negative (see above), but also because the maximal activatable current, which the depolarized voltages might have been expected to come closer to activating, was larger. Second, 10–100 μM 4-AP blocked most or all of the modulator-induced current also at the depolarized voltages (Fig. 12*A*, three fibers). Most importantly, however, we observed that the enhancement of the current by depolarization proceeded with characteristically slow kinetics. Thus, the net MM_A-, SCP_B-, or 5-HT-induced, and 4-AP–blocked, current increased gradually over several hundred milliseconds following the depolarizing voltage step (see particularly Fig. 12*Ac*; 22 fibers). This was in contrast to the much faster kinetics of the "A" and delayed-rectifier K currents that were also activated by the same voltage steps, and appeared to be unaltered by the modulators (see below). Once developed, the modulator-induced current did not undergo any voltage-dependent inactivation during depolarizations lasting as long as 5 sec (Fig. 12*B*).

The different postsynaptic modulators activate the K current in a mutually occlusive but otherwise noninteracting fashion

The very similar properties of the K currents activated by MM_A, SCP_B, and 5-HT (and presumably also MM_B and SCP_A) suggested that all of these postsynaptic modulators in fact activated the same current(s). If so, it might be possible to demonstrate mutual occlusion of the K-current responses to the different modulators.

Indeed, the small K currents activated by SCP_B, 5-HT, and MM_B exhibited clear mutual occlusion in many fibers. Thus, when a maximal concentration of one of these modulators (10–100 μM; see Fig. 3*C*) activated a substantial current, subsequent

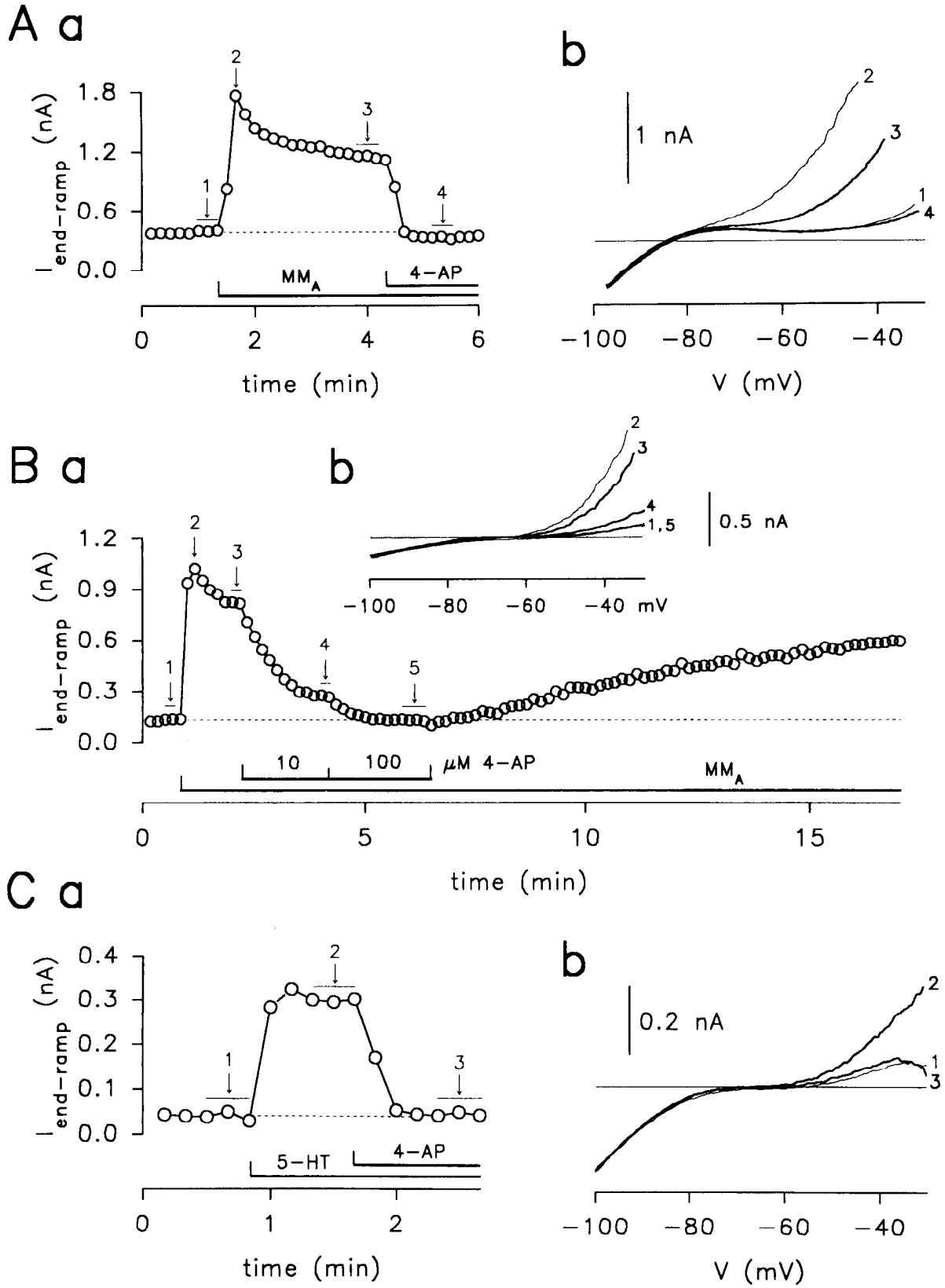

Figure 11. The modulator-induced K current is potently blocked by 4-AP. *I–V* relations were obtained with standard voltage ramps in normal ASW; in *A–C, a* is a plot of values of the absolute current at the end (the most positive voltage reached) of successive ramps, while *b* shows the complete *I–V* relations (each an average of up to four consecutive relations) obtained at the times indicated in *a*. *A*, 4-AP at 100 μM immediately blocks the K current activated by 10 μM MM_A. *B*, The current activated by 10 μM MM_A is blocked substantially by 10 μM and completely (in this experiment; see text) by 100 μM 4-AP; the block washes out slowly. *C*, 4-AP at 100 μM blocks completely also the K current activated by 10 μM 5-HT. Due to the slow washout of the 4-AP block, it was not possible in these experiments to test 4-AP also on the basal currents in the same fiber. Nevertheless, several considerations strongly suggested that practically all of the observed 4-AP effect represented selective block of the

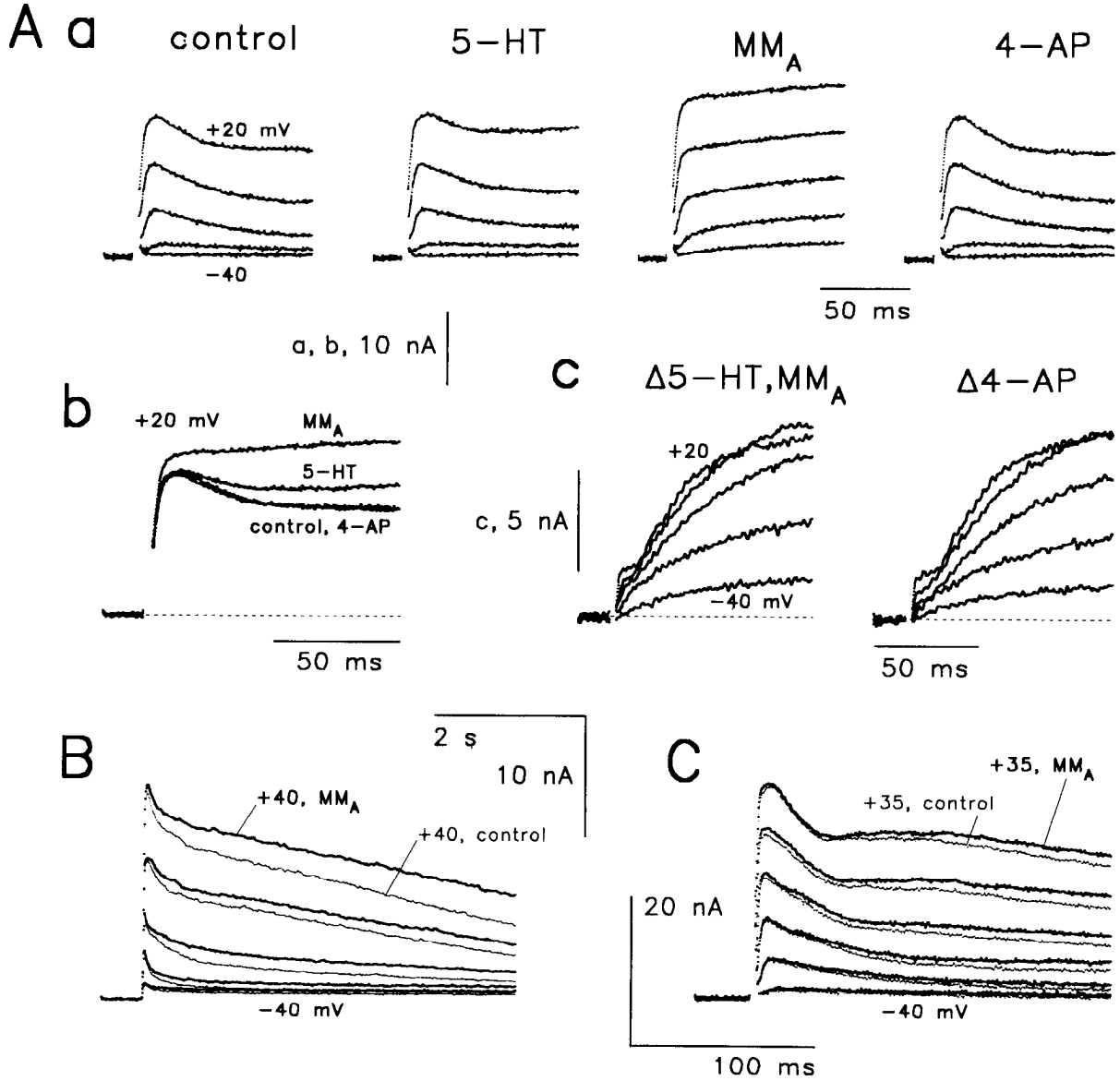

Figure 12. The modulator-induced K current turns on slowly upon depolarization. Currents were elicited by short (*A, C*) or long (*B*) voltage steps from a holding potential of −90 mV to a range of test potentials between −40 and +40 mV in normal ASW. *Aa,* Families of currents recorded under control conditions and then following cumulative application of 100 μM 5-HT, 10 μM MM_A, and finally 10 μM 4-AP. The currents elicited in each case by the step to the most positive test potential, +20 mV, have been superimposed for comparison in *Ab. Ac* shows families of difference records of the net current activated by 5-HT plus MM_A (*left*) and the net current blocked by 4-AP (*right*), obtained by subtracting respectively the *control* and the *4-AP* currents from the MM_A currents in *Aa.* Note the slow development of the modulator-induced, 4-AP–blocked current following the depolarizing step. *B,* Superimposed families of currents, recorded as in *Aa* but with long voltage steps, before (*thin traces*) and after (*thick traces*) application of 10 μM MM_A. The MM_A-induced current shows no voltage-dependent inactivation even at the end of the 5 sec depolarization. *C,* Experiment carried out as in *B,* but in a fiber in which the MM_A-induced current was unusually small relative to the preexisting depolarization-activated "A" and delayed-rectifier K currents (the early and late current peaks around 10 and 100 msec after the depolarizing step, respectively; see Figs. 2–6 of Březina et al., 1994b). These two K currents do not appear to be altered by the MM_A.

←

modulator-induced current, without any significant block of basal currents: (1) previously we found that, at the concentrations and voltages used here (up to 100 μM, more negative than −30 mV), 4-AP had virtually no effect on basal currents (see Fig. 1*B* of Březina et al., 1994b); in the present work, we found the same in experiments (described in the text) in which fibers were treated with 10–100 μM 4-AP prior to application of the modulators (15 fibers); (2) in any case, the basal outward currents even at −30 mV appeared in these fibers very small compared to the large amplitude of the modulator (particularly the MM_A)-induced current; (3) finally, in 100 μM 4-AP, not just the end-ramp current (*a* of *A–C*), but the whole shape of the *I–V* relation (*b* of *A–C*), as well as the characteristic time course of current elicited by a depolarizing voltage step (Fig. 12*A*), returned almost exactly to its premodulator state, unlikely if the 4-AP effect reflected a combined partial block of the modulator-induced and basal currents, and not complete, selective block solely of the modulator-induced current.

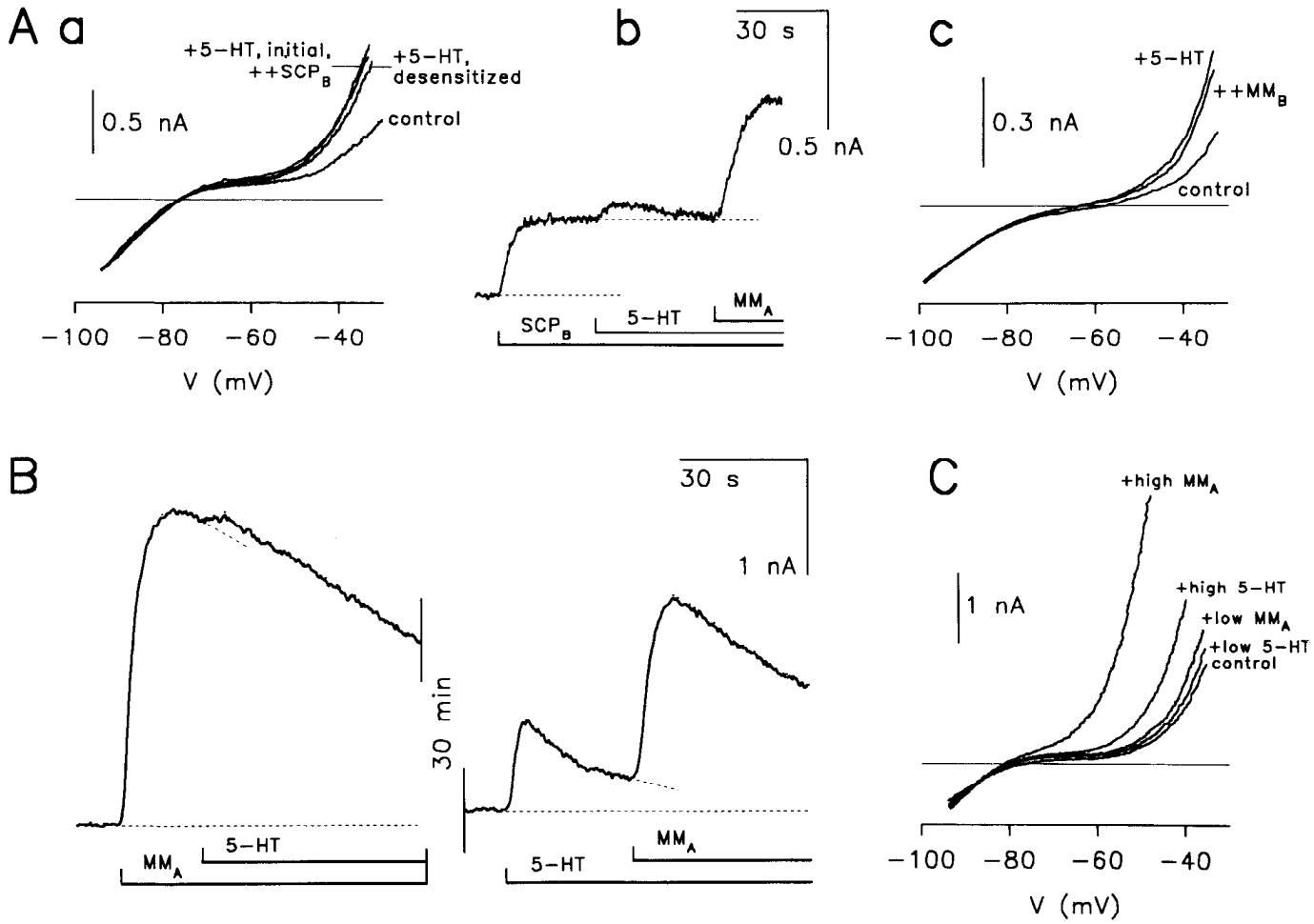

Figure 13. The different postsynaptic modulators activate the K current in a mutually occlusive but otherwise noninteracting fashion. *I–V* relations were obtained with standard voltage ramps (*Aa, Ac, C*), or the holding current at a steady −30 mV was monitored (*Ab, B*), all in normal ASW. Maximal (*A, B*) or submaximal (*C*) modulator concentrations were chosen from the dose–response relations in Figures 2 and 3. *A,* Examples of mutual occlusion of the small K currents activated by SCP_B, 5-HT, and MM_B. *Aa,* SCP_B at 10 μM has little additional effect when applied after 100 μM 5-HT (the 5-HT–induced current shows some desensitization). *Ab,* In the converse experiment, 100 μM 5-HT has little additional effect after 30 μM SCP_B; however, 10 μM MM_A activates additional current as usual. *Ac,* MM_B at 100 μM has no additional effect after 100 μM 5-HT. *B,* Under favorable circumstances (see text), the large MM_A-induced K current can be seen to occlude the small SCP_B- and 5-HT-induced currents. Here, 100 μM 5-HT has very little effect when applied at the peak of a large current activated by 10 μM MM_A; when, however, the modulators are applied (after a 30 min wash) in the reverse order, the 5-HT activates a substantial current which was presumably occluded in the first application. *C.* Combined application of submaximal concentrations of 5-HT and MM_A reveals no obvious synergism (even though subsequent application of maximal concentrations shows that the potential for a much larger response exists) or other alteration in the dose–response characteristics (compare Figs. 2, 3*B,C*) of their K-current effects. The modulators were cumulatively applied first at the *low* concentrations (100 nM 5-HT, then 10 nM MM_A), then the *high* concentrations (10 μM 5-HT, then 10 μM MM_A).

addition of even similarly high concentrations of one of the other two modulators often (though not always) had little or no further effect (Fig. 13*A*; 5-HT followed by SCP_B was tested in 14 fibers, SCP_B followed by 5-HT in eight fibers, 5-HT followed by MM_B in two fibers, MM_B followed by 5-HT in four fibers).

Due to the size disparity, it was more difficult to demonstrate mutual occlusion between the small currents and the large MM_A-induced K current. However, signs of occlusion were often present, and under certain favorable circumstances it was clearly evident: (1) Although, as already described, MM_A as a rule still had a substantial further effect even after maximal activation of the small currents, it nevertheless appeared that the MM_A-induced current was *partially* occluded. The further current activated by MM_A was, on average, smaller, compared to the current activated by MM_A alone, by roughly the amplitude of the current already activated by the other modulators; thus, the other modulators plus MM_A together activated about the same total amplitude of current as MM_A applied alone (compare Figs. 2*B*, 3*C*). (2) When occasionally one of the other modulators (most often 5-HT) activated an unusually large current more comparable in amplitude to the MM_A-induced current, the occlusion of the MM_A response was correspondingly more marked. (3) Finally, when, in one of these fibers with large 5-HT or SCP_B responses, we succeeded in at least partially washing out the modulators so as to be able to reapply them in the reverse order to obtain control measurements of the unoccluded currents in the same fiber, it was also clear that, conversely, the large MM_A-induced current occluded the small currents activated by 5-HT and SCP_B (Fig. 13*B*, 14 fibers).

Apart from the occlusion, however, we found no evidence of any interaction between the K-current responses to the different modulators. In particular, submaximal responses to 5-HT ap-

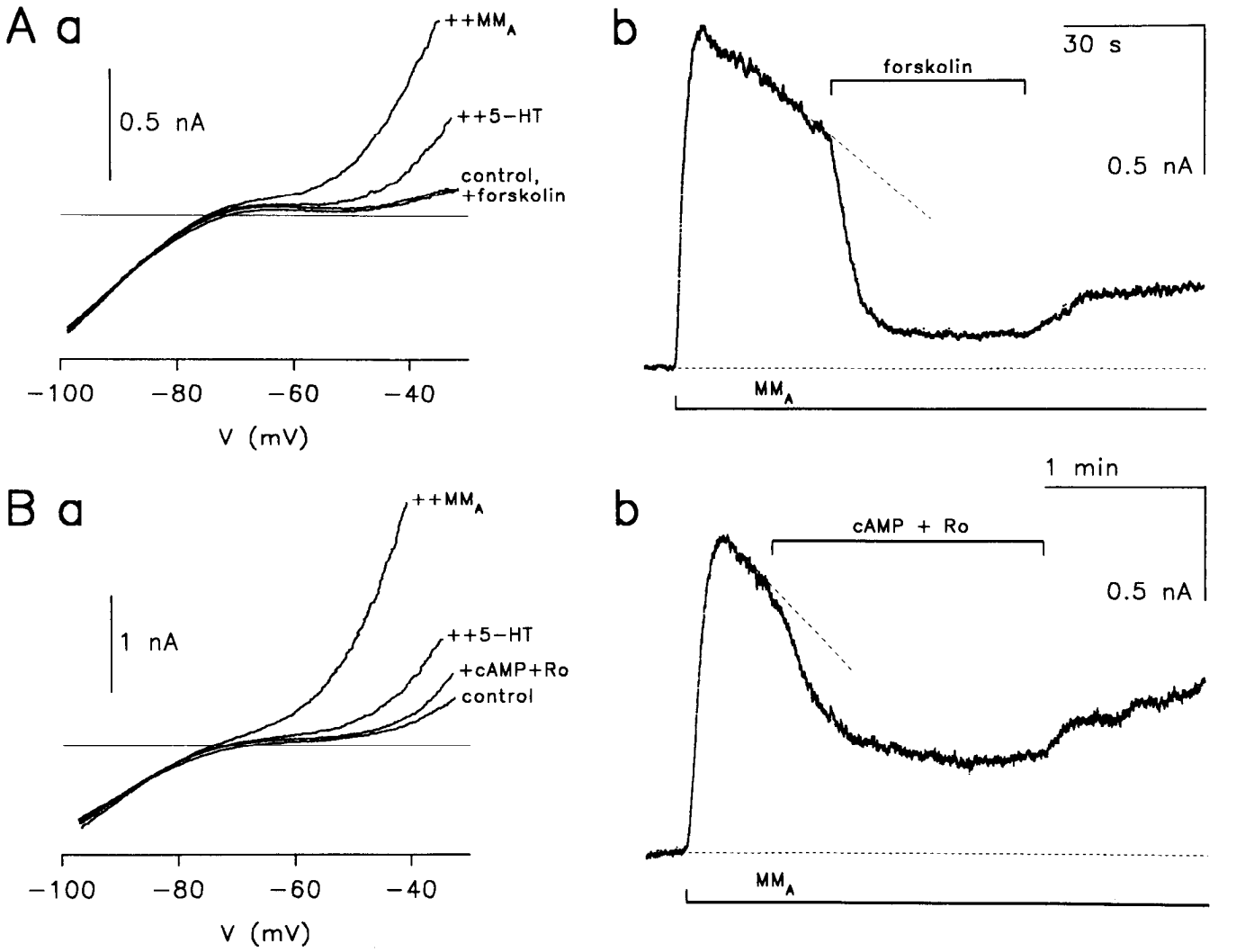

Figure 14. Forskolin and a cAMP analog fail to mimic—indeed, somewhat suppress—the K-current response to the modulators. *I–V* relations were obtained with standard voltage ramps (*Aa, Ba*), or the holding current at a steady −30 mV was monitored (*Ab, Bb*), all in normal ASW. *Aa,* Forskolin at 100 μM itself activates little or no K current, and apparently normal K currents are activated by 10 μM 5-HT followed by 10 μM MM_A in its presence. *Ab,* When 100 μM forskolin is applied after a large K current has already been activated by 10 μM MM_A, it reversibly suppresses it (*Aa* shows that its effect is not on the basal current). *B,* Similar results are obtained in experiments carried out as in *A* but with 1 mM CPT-cAMP plus 100 μM Ro 20-1724.

plied in combination with SCP_B, MM_A, or MM_B, and SCP_B combined with MM_A, were to a first approximation simply additive, rather than synergistic (Fig. 13*C*, five fibers). In the preceding article, we similarly found no interaction except for occlusion between the modulators' effects on the Ca current (Březina et al., 1994d).

cAMP does not activate the K current

In the preceding article, we confirmed that the postsynaptic modulators, at the concentrations used in our experiments, all elevated cAMP in the ARC muscle fibers; showed that elevation of cAMP with the adenylyl-cyclase activator forskolin or the cAMP analog 8-chlorophenylthio-cAMP (CPT-cAMP; applied in combination with the phosphodiesterase inhibitor Ro 20-1724) mimicked the modulator-induced enhancement of the "L"-type Ca current; and reviewed several lines of evidence suggesting that the enhancement of the Ca current and consequent potentiation of ARC-muscle contractions by the modulators is physiologically mediated by the cAMP second-messenger pathway (Březina et al., 1994d).

In contrast, the K-current responses of the modulators were not substantially mimicked by elevation of cAMP. We applied 100 μM forskolin (which indeed considerably elevated cAMP in the ARC muscle fibers: Fig. 2*b* of Březina et al., 1994d) or 1 mM CPT-cAMP plus 100 μM Ro 20-1724, the concentrations that we found to maximally enhance the Ca current (cf. Fig. 9 of Březina et al., 1994d). Both treatments occasionally activated a small outward current somewhat like the modulator-induced current (of about the same amplitude, interestingly, as its 4-AP–resistant fraction), but more often had no effect at all; in either case, all of the modulators continued to activate substantial (though possibly reduced; see next section) currents even in the presence of the cAMP-elevating agents (Fig. 14*Aa,Ba*; 11 fibers were tested with forskolin, five with CPT-cAMP plus Ro 20-1724). The small effect of forskolin, at least, was perhaps not

even due to its elevation of cAMP, as its "inactive" analog 1,9-dideoxyforskolin (which indeed failed to elevate cAMP in the ARC muscle fibers even at 100 μM; Fig. 2*b* of Březina et al., 1994d) acted similarly (two fibers).

Interestingly, we observed that, when either the forskolin or the CPT-cAMP plus Ro 20-1724 was applied after a large K current had already been activated by MM_A, both treatments reversibly suppressed the current (Fig. 14*Ab,Bb*; 14 and 6 fibers, respectively). This effect, too, could be reproduced with 1,9-dideoxyforskolin (five fibers). In view of this, together with the fact that MM_A itself elevated cAMP in the ARC muscle fibers no less than forskolin (Fig. 2*b* of Březina et al., 1994d), the fact that MM_A routinely activated large K currents in the presence of high 5-HT, SCP_A, and SCP_B (e.g., Figs. 3*B*, 4*B*, 8*B*), all of which elevated cAMP considerably *more* than forskolin (Fig. 2 of Březina et al., 1994d), as well as the lack of any effect on the MM_A-induced current by subsequently applied 5-HT or SCP_B (Fig. 13*B*), this suppression most likely represented a secondary, "pharmacological" effect of the forskolins as well as CPT-cAMP and/or Ro 20-1724. For the forskolins, at least, a number of such cAMP-independent actions have now been reported, including block of several K currents in molluscan neurons (Laurenza et al., 1989).

Receptor pharmacology

In the preceding article, we identified four compounds that have been reported to differentially block cAMP-linked effects of 5-HT in *Aplysia* neurons and muscle, and tested them in the ARC muscle fibers in the hope of similarly blocking the 5-HT–induced (and most likely cAMP-mediated) enhancement of the Ca current. Unfortunately, none of the compounds—ketanserin, ritanserin, cyproheptadine, and methysergide—proved useful (Březina et al., 1994d). The same was true for the K-current response to 5-HT. We applied ketanserin, ritanserin, and cyproheptadine at 10–100 μM and methysergide at up to 1 mM, sufficient concentrations according to the previous reports (for references, see Březina et al., 1994d). Although ketanserin (five fibers) and cyproheptadine (two fibers) both appeared to act as partial agonists, themselves activating some outward current especially at 100 μM, neither they nor ritanserin (four fibers) was able to prevent substantial additional effect of 1–10 μM 5-HT. Methysergide was a full agonist above 100 μM, and completely occluded the effect of 10–100 μM 5-HT (two fibers).

Other currents present in the ARC muscle fibers are not modulated

Previously (Březina et al., 1994a–c), we characterized five major ion currents present in the unmodulated ARC muscle fibers: two hyperpolarization-activated currents, an inwardly rectifying K current and a Cl current induced by elevated intracellular Cl^-; and three depolarization-activated currents, an "A" K current, a delayed-rectifier K current, and the "L"-type Ca current.

The modulator-induced K current was clearly different from all three preexisting K currents. Unlike the inward rectifier it was depolarization activated, yet its voltage dependence was not nearly as extreme as that of the "A" current or delayed rectifier; its activation kinetics were considerably slower than those of any of these currents; and it was much more sensitive to 4-AP (cf. Březina et al., 1994a,b). Indeed, the 4-AP insensitivity of the total preexisting current (see Fig. 1*B* of Březina et al., 1994b) argued against the idea that, as with the "L"-type Ca current, the modulators enhanced a component of preexisting current. Rather, it appeared that the modulator-induced K current was a new current truly *induced* by the modulators.

Of the preexisting currents, the preceding article described modulation of the "L"-type Ca current (Březina et al., 1994d). The other four preexisting currents, however, appeared not to be modulated. Thus, in the hundreds of experiments in which the modulators were tested on the *I–V* relations obtained with standard slow voltage ramps, even as they induced robust K currents in the depolarized portion of the standard-ramp voltage range, they had no consistent effect on the inward rectifier dominating its hyperpolarized portion. We saw no effect of up to 10 μM 5-HT (see, e.g., Figs. 7*B*, 11*Cb*, 13*Aa*, 14*Aa*), SCP_A, SCP_B (Fig. 13*Aa*), MM_A (Figs. 7*B*, 11*Ab*, 14*Aa*), or MM_B (Fig. 13*Ac*). [The presynaptic modulators $buccalins_{A,B,C}$ likewise had no effect (Fig. 4).] This was interesting, because the inward rectifier is well known to be enhanced by 5-HT, SCP, and other modulators acting via cAMP in a number of *Aplysia* neurons (Adams and Benson, 1985; Levitan et al., 1987; Lotshaw and Levitan, 1987a; Jansen and Mayeri, 1988; Kirk et al., 1988; Taussig et al., 1989), and, as already mentioned, the SCPs, MMs, and 5-HT all greatly elevated cAMP in the ARC muscle fibers (Březina et al., 1994d). Thus, the ARC-muscle inward rectifier appeared insensitive to cAMP. Indeed, it was unaffected also by up to 100 μM forskolin (Fig. 14*Aa*) or 1 mM CPT-cAMP plus 100 μM Ro 20-1724 (Fig. 14*Ba*).

The other hyperpolarization-activated current, the Cl current that turned on with very slow exponential kinetics following hyperpolarizing voltage steps in fibers Cl^- loaded by leakage from KCl-containing electrodes (Březina et al., 1994a), was also not affected by up to 10 μM of any of the modulators (two to eight fibers were tested with each modulator). Again, this was different from *Aplysia* neurons, where the Cl current has been reported to be decreased by 5-HT and forskolin (Lotshaw and Levitan, 1987b).

Finally, during the depolarizing voltage steps to positive potentials, when the modulator-induced K current was suppressed with 4-AP, the modulators appeared to have no significant effect on the preexisting "A" and delayed-rectifier K currents (best visible in Fig. 12*C*; 2–11 fibers were tested with up to 10 μM of each modulator).

Discussion

Identity of the modulator-induced K current(s)

In this article we have described a characteristic K current activated in the ARC muscle fibers by the postsynaptic modulators 5-HT, SCP_A, and SCP_B, and MM_A and MM_B (but not by the presynaptic modulators $buccalins_{A,B,C}$). The modulator-induced current is considerably enhanced by depolarization, but its voltage dependence is not as extreme as that of classical "voltage-dependent" K currents such as the "A" current and the delayed rectifier. Thus, the modulator-induced current is active to some extent even at the resting potential, indeed, particularly with the large currents induced by MM_A, even below E_K. Upon depolarization, the current increases with rather slow kinetics, over several hundred milliseconds. The current is Ca^{2+} independent, not readily blocked by extracellular Cs^+ or Ba^{2+} and only by high concentrations of TEA. However, it is almost completely blocked by as little as 10 μM 4-AP. One conceivable site of the 4-AP block, namely, at the receptor level, appears unlikely in view of the fact that 4-AP blocks equally currents activated presumably via at least three different receptors, re-

spectively, by the SCPs, MMs, and 5-HT. Furthermore, peptides of yet another family, the FMRFamide-related peptides (FRPs; Cropper et al., 1991b), clearly act via a different receptor from MM_A, yet activate the same K current, of comparable amplitude, and are equally well blocked by 4-AP (Březina and Weiss, 1993; unpublished observations). Thus, 4-AP presumably acts at a site downstream of the convergence of the pathways mediating the actions of the different modulators, most likely indeed directly on the K channels themselves.

The literature contains several reports of K currents that the modulator-induced current somewhat resembles in many of its properties including 4-AP sensitivity (e.g., Stansfeld et al., 1986; Storm, 1988; see also review by Rudy, 1988). However, such currents do not easily fit into any of the major classes of strongly voltage- or Ca^{2+}-dependent K currents (Rudy, 1988). Moreover, the modulator-induced current does not appear to be active except following exposure to the modulators. Thus, it might best be viewed as a slow "synaptic" current, albeit one with significant voltage dependence. Two subthreshold voltage-dependent K currents, whose modulation is well known to give rise to precisely such slow voltage-dependent synaptic currents, are the "M" current present in many vertebrate neurons (Brown et al., 1981; Jones and Adams, 1987; Brown, 1988) and the "S" current in *Aplysia* neurons (Klein et al., 1982; Shuster and Siegelbaum, 1987). The "S" current, in particular, is activated by FMRFamide (Belardetti et al., 1987; Březina et al., 1987; Critz et al., 1991) and, as already mentioned, FMRFamide and related peptides do indeed activate the modulator-induced current in the ARC muscle fibers (Březina and Weiss, 1993; unpublished observations). Furthermore, MM_A too has been reported to activate the "S" current in *Aplysia* sensory neurons (Critz et al., 1991). However, unlike the modulator-induced current, the "S" current is not affected by even 10 mM 4-AP (Shuster and Siegelbaum, 1987), while the "M" current is similarly 4-AP insensitive and furthermore is blocked by low-millimolar Ba^{2+} (Brown and Adams, 1980; Brown et al., 1981). Thus, the modulator-induced K current in the ARC muscle fibers is not identical to either the "S" or "M" current. Nevertheless, similarities in its voltage dependence and activation kinetics may lead to similar functional consequences (see below).

We have found that MM_A activates K currents of large amplitude while MM_B, SCP_A, SCP_B, and 5-HT, even at maximal concentrations, are able to activate only small currents. This difference in size has made it difficult to demonstrate conclusively that the large and small currents are in fact the same current. Nevertheless, their very similar properties and partial or complete occlusion make it probable that all of the postsynaptic modulators do indeed activate the same K current. Less clear is whether this current is homogeneous or contains two distinct components. Our 4-AP results are consistent with the possibility that, in addition to the large or small 4-AP–sensitive current, all of the modulators can activate also a very small component of 4-AP–resistant (but otherwise indistinguishable) current. However, such a small current might also have originated artifactually (see Results). Single-channel analysis will be required for a definitive accounting of the number of K currents activated by the postsynaptic modulators in the ARC muscle fibers.

Signal transduction mechanisms

We have found that, in contrast to the enhancement of the "L"-type Ca current (Březina et al., 1994d), activation of the K current is not substantially mimicked by elevation of cAMP. Thus, while the postsynaptic modulators very likely enhance the Ca current via the cAMP second-messenger pathway, this pathway probably does not mediate their K-current responses. This conclusion is supported by the finding that the FRPs activate large K currents even though they do not elevate cAMP in the ARC muscle (O. Harish, personal communication). At present we know nothing as to what other, if any, intracellular signal transduction mechanisms might be involved. In *Aplysia* neurons, activation of the "S" current by FMRFamide has been suggested to involve arachidonic acid metabolites and protein phosphatases (e.g., Piomelli et al., 1987; Critz et al., 1991; Endo et al., 1991; but see Březina, 1991). Future experiments will determine whether these pathways play any role in activating the K current in the ARC muscle.

In elevating cAMP in the ARC muscle fibers and enhancing the Ca current, MM_A and MM_B are approximately equally potent and efficacious (Březina et al., 1994d). In activating the K current, on the other hand, MM_A is considerably more efficacious than MM_B. The simplest explanation is that the Ca- and K-current effects are mediated by two different MM receptors. By analogy, this might also be true for the SCPs and 5-HT.

Modulation of the Ca and K currents as mechanisms of modulation of ARC-muscle contractions

Figure 15 graphically summarizes our present understanding of how the ARC muscle contracts, derived from our previous study of unmodulated fibers (Březina et al., 1994a–c), and our proposal of how the two actions of the postsynaptic modulators described in this and the preceding article, enhancement of the "L"-type Ca current and activation of the K current, might alter the contractions.

Physiologically, the ARC muscle contracts when it is sufficiently depolarized by ACh, the "classical" transmitter released by its two motor neurons B15 and B16. The muscle normally rests at a potential not far above E_K, and as it is depolarized follows a trajectory similar to the solid curve I_K in Figure 15 (this is the total current I–V relation of unstimulated ARC muscle fibers; during ACh-induced contraction it would be somewhat modified by addition of the ACh-induced current). Contraction begins above -40 or -35 mV, the activation threshold of the "L"-type Ca current that provides Ca^{2+} essential for the contraction (Březina and Weiss, 1993; Březina et al., 1994d). The ARC is a relatively slowly contracting, nonspiking muscle, in which the degree of contraction is directly determined by the membrane voltage (Cohen et al., 1978). The final voltage reached during strong sustained contraction is between -30 and -20 mV, set by superposition of the major currents active in that voltage range, the Ca current, the "A" and delayed-rectifier K currents, and the ACh-induced synaptic current, which reverses around -25 or -30 mV (Kozak et al., 1993; Březina et al., 1994b,c). Since at these voltages just above its threshold the Ca current increases very steeply with depolarization, small voltage changes provide fine control over a wide range of contraction strengths. Such voltage changes can be produced by varying cholinergic input, but equally by the actions of the postsynaptic modulators.

In the preceding article, we summarized evidence consistent with the idea that the enhancement of the "L"-type Ca current and thus of Ca^{2+} influx upon depolarization is the major mechanism by which all of the postsynaptic modulators examined here potentiate ARC-muscle contractions (Březina et al., 1994d).

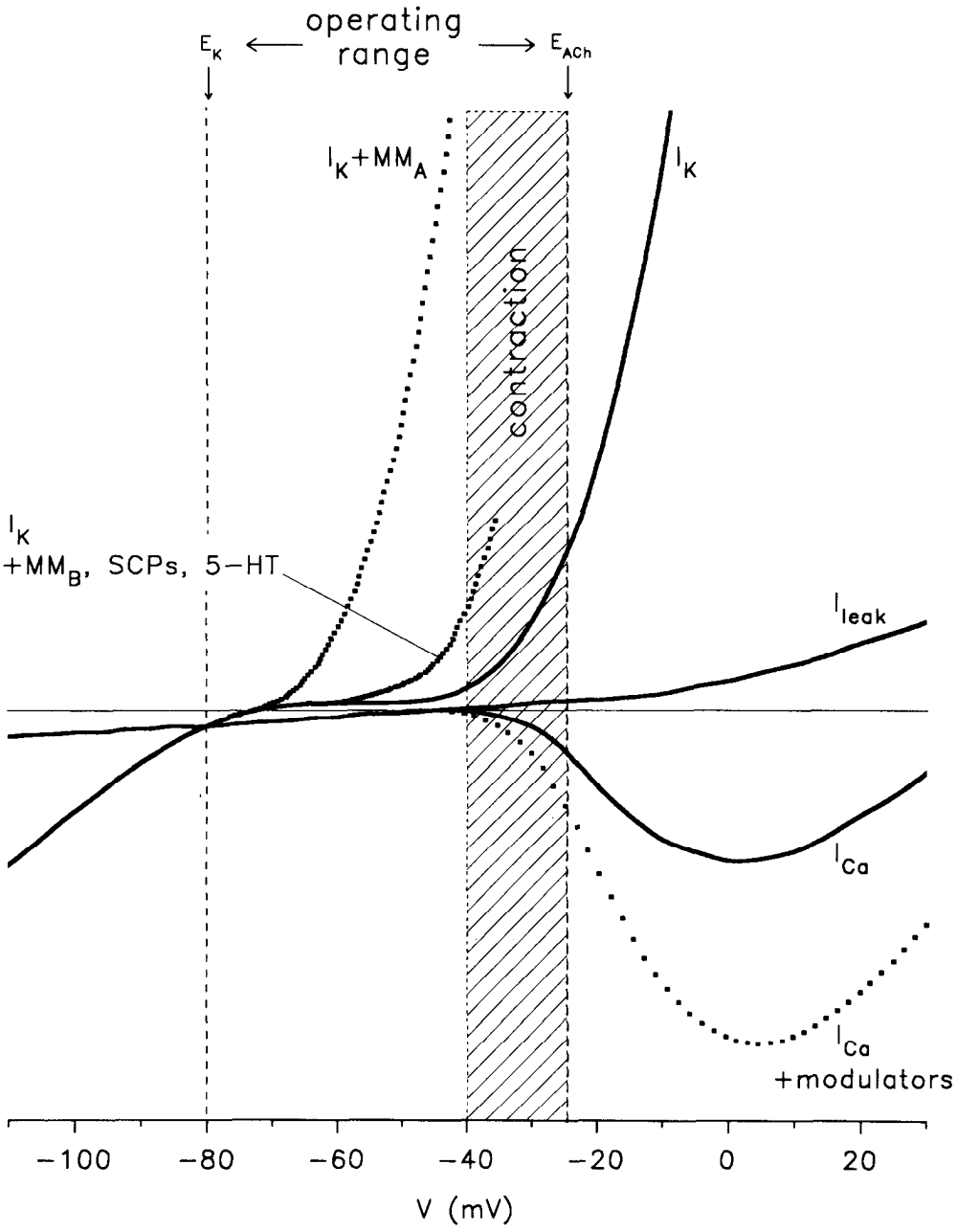

Figure 15. Schematic summary of the modulation of ARC-muscle currents described in this work and its proposed relation to contraction of the muscle. These representative schematic *I–V* relations were derived from actual experimental *I–V* relations obtained with slow voltage ramps. The *solid curves* I_K, I_{Ca}, and I_{leak}, representing different components of basal, unmodulated ARC-muscle current, are reproduced from Figure 9 of Březina et al. (1994c). I_K, *I–V* relation of total basal ARC-muscle current, dominated by the inwardly rectifying K current at negative voltages, the "A" and delayed-rectifier K currents at positive voltages, with the high-resistance plateau due to deactivation of the inward rectifier separating the two regions of rectification (see Březina et al., 1994a,b). I_{Ca}, *I–V* relation of the basal Ca current obtained when the K currents are blocked (Březina et al., 1994c). I_{leak}, *I–V* relation obtained when all major currents are blocked (Březina et al., 1994b). Superimposed on these basal *I–V* relations are the two types of postsynaptic modulation described in this and the preceding article (Březina et al., 1994d), activation of the small K current by the SCPs, 5-HT, and MM_B and of the large K current by MM_A, and enhancement of the Ca current by all of these modulators. E_K, K^+ equilibrium potential; E_{ACh}, reversal potential of ACh-induced current.

In contrast, activation of the K current, by adding an outward current to the superimposed currents determining the voltage reached during contraction, might be expected to shift that voltage in the hyperpolarized direction, limiting activation of the Ca current, Ca^{2+} influx, and thus contraction. We therefore propose activation of the K current as a mechanism by which the postsynaptic modulators, to different degrees, depress the ARC-muscle contractions. The depression is superimposed on the potentiation, as further discussed below.

Several observations already support our proposal. First, the ability of the various postsynaptic modulators to depress contractions is clearly correlated with the amplitude of K current they activate: the SCPs, 5-HT, and MM_B activate only small K currents and weakly depress contractions only at very high concentrations (Cropper, personal communication), whereas MM_A activates large currents and strongly depresses contractions already above 10^{-7} M (Cropper et al., 1991a). Similarly, the FRPs activate large currents and are potent depressors (Cropper et al., 1991b; Březina and Weiss, 1993). Second, preliminary results show that the hyperpolarizing action of the K current is both sufficient and necessary for the depression; when MM_A or the FRPs are applied under voltage clamp, even though they activate large K currents, they fail to depress contractions (Březina and Weiss, 1993). Finally, 4-AP, at the low concentrations at which it blocks the modulator-induced K current but no other current in the ARC muscle fibers, abolishes the depression of contractions by MM_A and the FRPs (Březina and Weiss, 1993).

The relatively slow activation of the modulator-induced K current upon depolarization may have functional significance. In other preparations, activation of currents with comparable voltage dependence and kinetics, including the "M" current (Brown et al., 1981; Jones and Adams, 1987) and according to

some reports the "S" current (Klein et al., 1982; Baxter and Byrne, 1989), often leads to accommodation, that is, progressive decrease in excitability and cessation of spiking elicited by steady depolarizing input (e.g., Klein et al., 1986; Madison and Nicoll, 1986; Stansfeld et al., 1986; Jones and Adams, 1987; Baxter and Byrne, 1990; Critz et al., 1991). The ARC muscle does not spike; nevertheless, when the motor neurons B15 and B16 fire in bursts (as they do physiologically) to give summating EJPs in and progressive development of contraction of the muscle (Cohen et al., 1978), one might expect an analogous greater depression of later than earlier EJPs, both because the K current has had more time to activate and because the later EJPs have summated to a more depolarized voltage where the current is larger. The result will be to permit the muscle to reach some steady level of contraction fast and then tend to clamp it there.

All of the modulators that we have examined here modulate to some extent both the Ca and the K current. Neglecting any presynaptic effects (cf. Vilim et al., 1992), their net effect on contraction will depend on the balance between the relative strengths of the modulation of the two currents. Thus, the SCPs, 5-HT, and MM_B are predominantly potentiators because they strongly enhance the Ca current but only weakly activate the K current. The FRPs are depressors because they strongly activate the K current but do not enhance the Ca current (unpublished observations). MM_A acts strongly on both currents and thus will simultaneously potentiate and depress the contractions. The potentiation predominates at lower and the depression at higher MM_A concentrations (Cropper et al., 1991a). However, the concentrations at which MM_A acts on the two currents are not very different (compare Fig. 2*B* of this article with Fig. 6*B* of the preceding article); thus, most likely, when contractions are potentiated by even the lowest MM_A concentrations, they are at the same time already also somewhat depressed. Conversely, when contractions are profoundly depressed by higher MM_A concentrations, an underlying potentiation is revealed when the depression is eliminated by 4-AP or under voltage clamp, confirming that both mechanisms are operating simultaneously in the same fiber (Březina and Weiss, 1993). The asymmetry between potentiation and depression may reflect the fact that the two mediating mechanisms are not symmetrically opposed: as Figure 15 shows, activation of a sufficiently large K current will negate even the strongest enhancement of the Ca current by clamping depolarization below the activation threshold of the Ca channels, thus entirely arresting contractions (cf. Cropper et al., 1991a).

In the preceding article, we noted that modulation of Ca current has been found to be a mechanism by which contractions are modulated in many other muscle types. The same is true of K currents, which regulate, often in much the same manner as we have proposed here, contractility of, for example, vertebrate cardiac (Löffelholz and Pappano, 1985; Pennefather and Cohen, 1990) and smooth muscle (e.g., Bülbring and Tomita, 1987; Standen et al., 1989; Nelson et al., 1990; Brayden and Nelson, 1992; Escande and Cavero, 1992; Weston and Edwards, 1992). In invertebrates, too, contractions of numerous muscles have been reported to be potentiated and depressed very much as those of the ARC muscle, often by the very same modulators similarly released at the neuromuscular junction or circulating as hormones (e.g., Kravitz et al., 1980, 1985; Lloyd, 1980; Muneoka and Kamura, 1982; Evans and Myers, 1986; Hirata et al., 1989; Zoran et al., 1989; Lotshaw and Lloyd, 1990; Muneoka et al., 1991; Church et al., 1993; reviewed by Calabrese, 1989). Modulatory mechanisms like those in the ARC muscle may thus be ubiquitous.

In summary, we have in this and the preceding article reported that the SCPs, MMs, and 5-HT enhance the "L"-type Ca current and activate a K current so as to, we propose, respectively potentiate and depress contractions of the ARC muscle of *Aplysia*. We are now carrying out experiments (for preliminary report see Březina and Weiss, 1993) combining current and voltage clamp with simultaneous on-line length measurement of the dissociated fibers in order to evaluate directly the contribution of the modulation of the currents to the modulation of contractions.

References

Adams WB, Benson JA (1985) The generation and modulation of endogenous rhythmicity in the *Aplysia* bursting pacemaker neurone R15. Prog Biophys Mol Biol 46:1–49.

Baxter DA, Byrne JH (1989) Serotonergic modulation of two potassium currents in the pleural sensory neurons of *Aplysia*. J Neurophysiol 62:665–679.

Baxter DA, Byrne JH (1990) Differential effects of cAMP and serotonin on membrane current, action-potential duration, and excitability in somata of pleural sensory neurons of *Aplysia*. J Neurophysiol 64:978–990.

Belardetti F, Kandel ER, Siegelbaum SA (1987) Neuronal inhibition by the peptide FMRFamide involves opening of S K^+ channels. Nature 325:153–156.

Brayden JE, Nelson MT (1992) Regulation of arterial tone by activation of calcium-dependent potassium channels. Science 256:532–535.

Březina V (1991) On the role of arachidonic acid and its metabolites as second messengers modulating ion channel activity in *Aplysia* neurons. In: Molluscan neurobiology (Kits KS, Boer HH, Joosse J, eds), pp 123–130. Amsterdam: North-Holland.

Březina V, Weiss KR (1993) Analysis of ion currents mediating modulation of contractions of the ARC muscle of *Aplysia* by simultaneous on-line length measurement and current/voltage clamp. Soc Neurosci Abstr 19:1262.

Březina V, Eckert R, Erxleben C (1987) Modulation of potassium conductances by an endogenous neuropeptide in neurones of *Aplysia californica*. J Physiol (Lond) 382:267–290.

Březina V, Cropper EC, Evans CG, Kupfermann I, Weiss KR (1992) Enhancement of Ca and K currents by modulatory peptide cotransmitters correlated with potentiation and depression of contractions of the ARC muscle of *Aplysia*. Soc Neurosci Abstr 18:586.

Březina V, Evans CG, Weiss KR (1994a) Characterization of the membrane ion currents of a model molluscan muscle, the accessory radula closer muscle of *Aplysia californica*. I. Hyperpolarization-activated currents. J Neurophysiol, in press.

Březina V, Evans CG, Weiss KR (1994b) Characterization of the membrane ion currents of a model molluscan muscle, the accessory radula closer muscle of *Aplysia californica*. II. Depolarization-activated K currents. J Neurophysiol, in press.

Březina V, Evans CG, Weiss KR (1994c) Characterization of the membrane ion currents of a model molluscan muscle, the accessory radula closer muscle of *Aplysia californica*. III. Depolarization-activated Ca current. J Neurophysiol, in press.

Březina V, Evans CG, Weiss KR (1994d) Enhancement of Ca current in the accessory radula closer muscle of *Aplysia californica* by neuromodulators that potentiate its contractions. J Neurosci 14:4393–4411.

Brown DA (1988) M-currents: an update. Trends Neurosci 11:294–299.

Brown DA, Adams PR (1980) Muscarinic suppression of a novel voltage-sensitive K^+ current in a vertebrate neurone. Nature 283: 673–676.

Brown DA, Constanti A, Adams PR (1981) Slow cholinergic and peptidergic transmission in sympathetic ganglia. Fed Proc 40:2625–2630.

Bülbring E, Tomita T (1987) Catecholamine action on smooth muscle. Pharmacol Rev 39:49–96.

Calabrese RL (1989) Modulation of muscle and neuromuscular junctions in invertebrates. Semin Neurosci 1:25–34.

Church PJ, Whim MD, Lloyd PE (1993) Modulation of neuromuscular transmission by conventional and peptide transmitters released from excitatory and inhibitory motor neurons in *Aplysia*. J Neurosci 13:2790–2800.

Cohen JL, Weiss KR, Kupfermann I (1978) Motor control of buccal muscles in *Aplysia*. J Neurophysiol 41:157–180.

Critz SD, Baxter DA, Byrne JH (1991) Modulatory effects of serotonin, FMRFamide, and myomodulin on the duration of action potentials, excitability, and membrane currents in tail sensory neurons of *Aplysia*. J Neurophysiol 66:1912–1926.

Cropper EC, Lloyd PE, Reed W, Tenenbaum R, Kupfermann I, Weiss KR (1987a) Multiple neuropeptides in cholinergic motor neurons of *Aplysia*: evidence for modulation intrinsic to the motor circuit. Proc Natl Acad Sci USA 84:3486–3490.

Cropper EC, Tenenbaum R, Kolks MAG, Kupfermann I, Weiss KR (1987b) Myomodulin: a bioactive neuropeptide present in an identified cholinergic buccal motor neuron of *Aplysia*. Proc Natl Acad Sci USA 84:5483–5486.

Cropper EC, Miller MW, Tenenbaum R, Kolks MAG, Kupfermann I, Weiss KR (1988) Structure and action of buccalin: a modulatory neuropeptide localized to an identified small cardioactive peptide-containing cholinergic motor neuron of *Aplysia californica*. Proc Natl Acad Sci USA 85:6177–6181.

Cropper EC, Miller MW, Vilim FS, Tenenbaum R, Kupfermann I, Weiss KR (1990) Buccalin is present in the cholinergic motor neuron B16 of *Aplysia* and it depresses accessory radula closer muscle contractions evoked by stimulation of B16. Brain Res 512:175–179.

Cropper EC, Vilim FS, Alevizos A, Tenenbaum R, Kolks MAG, Rosen S, Kupfermann I, Weiss KR (1991a) Structure, bioactivity, and cellular localization of myomodulin B: a novel *Aplysia* peptide. Peptides 12:683–690.

Cropper EC, Vilim F, Vitek A, Miller MW, Kupfermann I, Weiss KR (1991b) RFa peptides are present in the ARC neuromuscular system of *Aplysia*. Soc Neurosci Abstr 17:1305.

Endo S, Ichinose M, Critz SD, Eskin A, Byrne JH, Shenolikar S (1991) Protein phosphatases and their role in control of membrane currents in *Aplysia* neurons. Adv Prot Phosphatases 6:411–432.

Escande D, Cavero I (1992) K^+ channel openers and "natural" cardioprotection. Trends Pharmacol Sci 13:269–272.

Evans PD, Myers CM (1986) Peptidergic and aminergic modulation of insect skeletal muscle. J Exp Biol 124:143–176.

Hirata T, Kubota I, Iwasawa N, Fujisawa Y, Muneoka Y, Kobayashi M (1989) Effects of *Mytilus* inhibitory peptides on mechanical responses of various molluscan muscles. Comp Biochem Physiol 93C: 381–388.

Jansen RF, Mayeri E (1988) The neuropeptide egg-laying hormone modulates multiple ionic currents in single target neurons of the abdominal ganglion of *Aplysia*. J Neurosci 8:3074–3084.

Jones SW, Adams PR (1987) The M-current and other potassium currents of vertebrate neurons. In: Neuromodulation (Kaczmarek LK, Levitan IB, eds), pp 159–186. New York: Oxford UP.

Kirk MD, Taussig R, Scheller RH (1988) Egg-laying hormone, serotonin, and cyclic nucleotide modulation of ionic currents in the identified motoneuron B16 of *Aplysia*. J Neurosci 8:1181–1193.

Klein M, Camardo J, Kandel ER (1982) Serotonin modulates a specific potassium current in the sensory neurons that show presynaptic facilitation in *Aplysia*. Proc Natl Acad Sci USA 79:5713–5717.

Klein M, Hochner B, Kandel ER (1986) Facilitatory transmitters and cAMP can modulate accommodation as well as transmitter release in *Aplysia* sensory neurons: evidence for parallel processing in a single cell. Proc Natl Acad Sci USA 83:7994–7998.

Kozak JA, Weiss KR, Březina V (1993) Acetylcholine activates two currents in the ARC muscle of *Aplysia*. Soc Neurosci Abstr 19:744.

Kravitz EA, Glusman S, Harris-Warrick RM, Livingstone MS, Schwarz T, Goy MF (1980) Amines and a peptide as neurohormones in lobsters: actions on neuromuscular preparations and preliminary behavioural studies. J Exp Biol 89:159–175.

Kravitz EA, Beltz B, Glusman S, Goy M, Harris-Warrick R, Johnston M, Livingstone M, Schwarz T, Siwicki KK (1985) The well-modulated lobster: the roles of serotonin, octopamine, and proctolin in the lobster nervous system. In: Model neural networks and behavior (Selverston AI, ed), pp 339–360. New York: Plenum.

Laurenza A, Sutkowski EM, Seamon KB (1989) Forskolin: a specific stimulator of adenylyl cyclase or a diterpene with multiple sites of action? Trends Pharmacol Sci 10:442–447.

Levitan ES, Kramer RH, Levitan IB (1987) Augmentation of bursting pacemaker activity by egg-laying hormone in *Aplysia* neuron R15 is mediated by a cyclic AMP-dependent increase in Ca^{2+} and K^+ currents. Proc Natl Acad Sci USA 84:6307–6311.

Lloyd PE (1980) Modulation of neuromuscular activity by 5-hydroxytryptamine and endogenous peptides in the snail, *Helix aspersa*. J Comp Physiol 139:333–339.

Lloyd PE, Kupfermann I, Weiss KR (1984) Evidence for parallel actions of a molluscan neuropeptide and serotonin in mediating arousal in *Aplysia*. Proc Natl Acad Sci USA 81:2934–2937.

Löffelholz K, Pappano AJ (1985) The parasympathetic neuroeffector junction of the heart. Pharmacol Rev 37:1–24.

Lotshaw DP, Levitan IB (1987a) Serotonin and forskolin increase and inwardly rectifying potassium conductance in cultured identified *Aplysia* neurons. J Neurophysiol 58:909–921.

Lotshaw DP, Levitan IB (1987b) Serotonin and forskolin modulation of a chloride conductance in cultured identified *Aplysia* neurons. J Neurophysiol 58:922–939.

Lotshaw DP, Lloyd PE (1990) Peptidergic and serotonergic facilitation of a neuromuscular synapse in *Aplysia*. Brain Res 526:81–94.

Madison DV, Nicoll RA (1986) Actions of noradrenaline recorded intracellularly in rat hippocampal CA1 pyramidal neurones, *in vitro*. J Physiol (Lond) 372:221–244.

Miller MW, Beushausen S, Cropper EC, Eisinger K, Stamm S, Vilim FS, Vitek A, Zajc A, Kupfermann I, Brosius J, Weiss KR (1993) The buccalin-related neuropeptides: isolation and characterization of an *Aplysia* cDNA clone encoding a family of peptide cotransmitters. J Neurosci 13:3346–3357.

Muneoka Y, Kamura M (1982) The multiplicity of neurotransmitters and neurohormones controlling *Mytilus* muscle. Comp Biochem Physiol 73C:149–156.

Muneoka Y, Fujisawa Y, Matsuura M, Ikeda T (1991) Neurotransmitters and neuromodulators controlling the anterior byssus retractor muscle of *Mytilus edulis*. Comp Biochem Physiol 98C:105–114.

Nelson MT, Huang Y, Brayden JE, Hescheler J, Standen NB (1990) Arterial dilations in response to calcitonin gene-related peptide involve activation of K^+ channels. Nature 344:770–773.

Pennefather P, Cohen IS (1990) Molecular mechanisms of cardiac K^+-channel regulation. In: Cardiac electrophysiology: from cell to bedside (Zipes DP, Jalife J, eds), pp 17–28. Philadelphia: Saunders.

Piomelli D, Volterra A, Dale N, Siegelbaum SA, Kandel ER, Schwartz JH, Belardetti F (1987) Lipoxygenase metabolites of arachidonic acid as second messengers for presynaptic inhibition of *Aplysia* sensory cells. Nature 328:38–43.

Rudy B (1988) Diversity and ubiquity of K channels. Neuroscience 25:729–749.

Shuster MJ, Siegelbaum SA (1987) Pharmacological characterization of the serotonin-sensitive potassium channel of *Aplysia* sensory neurons. J Gen Physiol 90:587–608.

Standen NB, Quayle JM, Davies NW, Brayden JE, Huang Y, Nelson MT (1989) Hyperpolarizing vasodilators activate ATP-sensitive K^+ channels in arterial smooth muscle. Science 245:177–180.

Stansfeld CE, Marsh SJ, Halliwell JV, Brown DA (1986) 4-Aminopyridine and dendrotoxin induce repetitive firing in rat visceral sensory neurones by blocking a slowly inactivating outward current. Neurosci Lett 64:299–304.

Storm JF (1988) Temporal integration by a slowly inactivating K^+ current in hippocampal neurons. Nature 336:379–381.

Taussig R, Sweet-Cordero A, Scheller RH (1989) Modulation of ionic currents in *Aplysia* motor neuron B15 by serotonin, neuropeptides, and second messengers. J Neurosci 9:3218–3229.

Vilim FS, Price DA, Kupfermann I, Weiss KR (1992) Modulation of peptide co-transmitter release from B15 neuromuscular junctions of *Aplysia*. Soc Neurosci Abstr 18:1104.

Weiss KR, Cohen JL, Kupfermann I (1978) Modulatory control of buccal musculature by a serotonergic neuron (metacerebral cell) in *Aplysia*. J Neurophysiol 41:181–203.

Weston AH, Edwards G (1992) Recent progress in potassium channel opener pharmacology. Biochem Pharmacol 43:47–54.

Zoran MJ, Haydon PG, Matthews PJ (1989) Aminergic and peptidergic modulation of motor function at an identified neuromuscular junction in *Helisoma*. J Exp Biol 142:225–243.